Received: 29 May 2020 | Revised: 12 October 2020 | Accepted: 12 October 2020

DOI: 10.1002/dneu.22786

Check for updates

RESEARCH ARTICLE

WILEY

Migration and fate of vestibular melanocytes during the development of the human inner ear

Edward S. A. van Beelen | **Wouter H. van der Valk** | **John C. M. J. de Groot** | **Erik F. Hensen** | **Heiko Locher** | **Peter Paul G. van Benthem**

Department of Otorhinolaryngology and Head & Neck Surgery, Leiden University Medical Center, Leiden, the Netherlands

Correspondence
Heiko Locher, Department of Otorhinolaryngology and Head & Neck Surgery, Leiden University Medical Center, Building 1, Room H05-40, P.O. Box 9600, 2300 RC, Leiden, the Netherlands.
Email: H.Locher@lumc.nl

Funding information
Hoogenboom-Beckfonds foundation

Abstract

Melanocytes are present in various parts of the inner ear, including the stria vascularis in the cochlea and the dark cell areas in the vestibular organs, where they contribute to endolymph homeostasis. Developmental studies describing the distribution of vestibular melanocytes are scarce, especially in humans. In this study, we investigated the distribution and maturation of the vestibular melanocytes in relation to the developing dark cell epithelium in inner ear specimens from week 5 to week 14 of development and in surgical specimens of the adult ampulla. Vestibular melanocytes were located around the utricle and the ampullae of the semicircular canals before week 7 and were first seen underneath the transitional zones and dark cell areas between week 8 and week 10. At week 10, melanocytes made intimate contact with epithelial cells, interrupting the local basement membrane with their dendritic processes. At week 11, most melanocytes were positioned under the dark cell epithelia. No melanocytes were seen around or in the saccule during all investigated developmental stages. The dark cell areas gradually matured and showed an adult immunohistochemical profile of the characteristic ion transporter protein Na^+/K^+-ATPase α1 by week 14. Furthermore, we investigated the expression of the migration-related proteins ECAD, PCAD, KIT, and KITLG in melanocytes and dark cell epithelium. This is the first study to describe the spatiotemporal distribution of vestibular melanocytes during the human development and thereby contributes to understanding normal vestibular function and pathophysiological mechanisms underlying vestibular disorders.

KEYWORDS

embryonic and fetal development, inner ear, melanocytes, saccule and utricle, vestibular labyrinth

1 | INTRODUCTION

The inner ear of humans and other mammals is contained within the temporal bone. It comprises the cochlea and the vestibular organs, which are involved in sound perception and spatial orientation and balance, respectively. Apart from these sensory systems, the inner ear contains a number of diverse accessory cells, among which are pigment-containing

This is an open access article under the terms of the Creative Commons Attribution-NonCommercial License, which permits use, distribution and reproduction in any medium, provided the original work is properly cited and is not used for commercial purposes.
© The Authors. *Developmental Neurobiology* published by 2020 Wiley Periodicals LLC

melanocytes. The existence of pigment in the inner ear has long been known. It was first described in 1851 by the Italian physician and early pioneer of inner ear microanatomy Alfonso Corti, but it took 80 years before the pigment was identified as melanin (Wolf, 1931). Studies investigating the function of melanocytes in mice unraveled their role in generation of the endocochlear potential and hearing (Hilding & Ginzberg, 1977; Igarashi, 1989; Schrott & Spoedlin, 1987; Steel & Barkway, 1989; Steel et al., 1987) and balance (Marcus & Wangemann, 2010; Palma et al., 2018). The functional importance of melanocytes for hearing and balance is also suggested by the wide dispersion of this cell type within the inner ear: melanocytes can be found in the cochlea, the vestibular organs (utricle, saccule, and the semicircular canals), and the endolymphatic sac (Figure 1), not only in humans and pigmented animal species but also in albino animal species (see also Table S1 for an extensive list on literature describing locations of melanocytes in the mammalian inner ear).

In the cochlea, melanocytes are most conspicuous in the stria vascularis in which they form the intermediate cell layer. Melanocytes have also been observed in other parts and tissues of the cochlea: they have been identified within the spiral ligament (LaFerriere et al., 1974; Savin, 1965; Wright & Lee, 1989), the modiolus, and the osseous spiral lamina (Franz et al., 1990; Glueckert et al., 2018; Roberts & Linthicum, 2015; Savin, 1965; Wolf, 1931), in Reissner's membrane (De Fraissinette et al., 1993; Felix et al., 1993; Glueckert et al., 2018; Savin, 1965), and in the basilar membrane (Glueckert et al., 2018; Roberts & Linthicum, 2015; Savin, 1965).

In the vestibular system, melanocytes can be found in the dark cell area of the utricle and the ampullae of the semicircular canals ([Figure 1; Coppens et al., 2004; Escobar et al., 1995; Igarashi, 1989; Igarashi et al., 1989; LaFerriere et al., 1974; Masuda et al., 1994, 1995, 1997; Okuno & Nomura, 1996; Palma et al., 2018). Dark cell epithelium and subepithelial melanocytes are functionally comparable to the marginal and intermediate cells of the stria vascularis, respectively, and are essential for endolymph homeostasis (Ciuman, 2009; Marcus et al., 2002; Wangemann, 2002). The majority of the vestibular subepithelial melanocytes is closely aligned with the dark cell

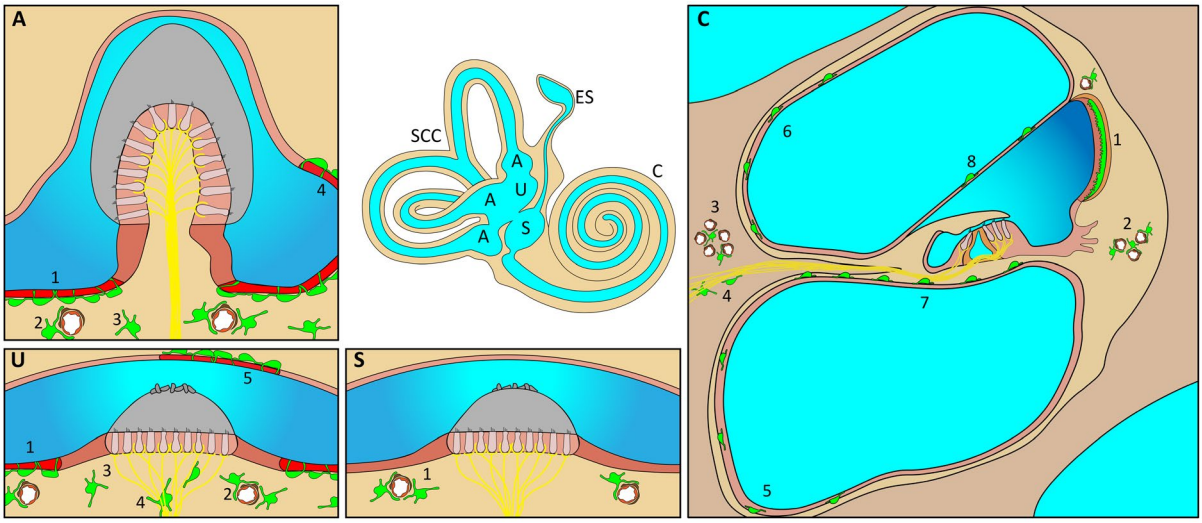


FIGURE 1 Schematic overview of melanin-containing cells in the mammalian inner ear. Melanin-containing cells (melanocytes, melanophages, and perivascular-resident macrophage-like melanocytes cells; all in green) are present in the vestibular organs (U, S, and A), the cochlea (C), and the endolymphatic sac (ES). A: Cross-section of the ampulla of a semicircular canal (SSC). Subepithelial melanocytes (1) are present underneath the dark cell epithelium (red). Also, perivascular-resident macrophage-like melanocytes (2) and subepithelial melanophages (3) are present in the subepithelial connective tissue. Subepithelial melanocytes are also associated with the dark cell epithelium in the area of the ampullar roof that connects to the opening of the utricle (4). In the semicircular canal proper (not shown), subepithelial melanocytes are present within the loosely arranged connective tissue of the periotic (perilymphatic) spaces. U: Cross-section of the utricle. Subepithelial melanocytes (1) are associated with the dark cell epithelium (red). Perivascular-resident macrophage-like melanocytes (2) and subepithelial melanophages (3) are present in the subepithelial connective tissue as well as perineural melanocytes (4) surrounding the nerve fibers. Subepithelial melanocytes are also associated with the dark cell epithelium in the utricular roof (5). S: Cross-section of the saccule. Perivascular-resident macrophage-like melanocytes (1) are present in the subepithelial connective tissue. C: Cross-section of a quarter turn of the cochlea. In the lateral wall, intermediate cells, and perivascular-resident macrophage-like melanocytes are present in the stria vascularis (1). In the spiral ligament, perivascular melanocytes are mainly located in the region superior and inferior to the stria vascularis (2). In the modiolus, perivascular (3) and perineural (4) melanocytes are present. Additionally, melanocytes are interspersed among the mesothelial cells in the modiolar wall facing the scala tympani (5) and scala vestibuli (6). Melanocytes are also present between the basement membrane and mesothelial cells of the tympanic covering layer of the osseous spiral lamina and basilar membrane (7), and on the mesothelial side of the basement membrane of the Reissner's membrane (8)

epithelium. Melanocytes have dendritic processes that protrude through the basement membrane and make direct contact with dark cells, similar to the strial melanocytes which interact with the marginal cells. In addition, vestibular melanocytes are present in the subepithelial connective tissue of the utricular and ampullar roofs (Kikuchi et al., 1994; Kimura, 1969) and show a close association with capillaries (Escobar et al., 1995; Igarashi et al., 1989; LaFerriere et al., 1974; Masuda et al., 1997; Zhang et al., 2013). Although the dark cell epithelium is not present in the saccule and the semicircular canals, melanocytes can still be found at these locations, diffusely distributed throughout the subepithelial connective tissue underlying the single epithelial lining of the extramacular regions of the saccule and semicircular canals (Coppens et al., 2004; Kim et al., 2019; Kimura, 1969; LaFerriere et al., 1974; Masuda et al., 1996; Wolf, 1931). In addition, melanocytes are present in the perisaccular connective tissue surrounding the intraosseous part (pars rugosa) of the endolymphatic sac (Fukazawa et al., 1993, 1994; Gussen, 1978).

The significance of inner ear melanocytes is clinically apparent as well. Both in animals and humans, sensorineural hearing loss and vestibular disorders can be associated with anomalies of pigmentation, either as associated symptoms of disease or manifestations of a syndrome. Examples include Vogt–Koyanagi–Harada disease, Waardenburg syndrome, Tietz syndrome, and Yemenite deaf-blind syndrome (for a review, see Lavezzo et al., 2016; Pingault et al., 2010). In addition, audiovestibular disorders are seen in patients with vitiligo and melanoma (Barozzi et al., 2015).

During the development, inner ear melanocytes differentiate from multipotent stem cells that originate and delaminate from the neural crest after closure of the neural tube (Cable & Steel, 1991; Freyer et al., 2011; Schrott & Spoedlin, 1987; Steel et al., 1987; Steel & Barkway, 1989; Wakaoka et al., 2013). The majority of developmental studies on inner ear tissues have been performed in laboratory animals. Descriptive studies about the distribution and morphology of vestibular melanocytes during human embryonic and fetal development are scarce. Previously, our group studied cochlear melanocytes and their incorporation into the stria vascularis during the human inner ear development (Locher et al., 2015). In the present study, we address for the first time the developmental distribution of human vestibular melanocytes following delamination from the neural crest to the moment of their subepithelial localization underneath the dark cells, using human embryonic, fetal, and adult specimens.

2 | MATERIALS AND METHODS

2.1 | Ethics statement

Use of human embryonic and fetal specimens was in accordance with Dutch legislation (Fetal Tissue Act, 2001) and the WMA Declaration of Helsinki guidelines, and approval for this project was obtained from the Medical Research Ethics Committee of Leiden University Medical Center (protocol registration number B18.044). Written informed consent of the donor was obtained following the Guidelines on the Provision of Fetal Tissue set by the Dutch Ministry of Health, Welfare, and Sport (revised version, 2018). Collection of adult vestibular tissue harvested during translabyrinthine vestibular schwannoma surgery was approved by the Medical Research Ethics Committee of Leiden University Medical Center (protocol registration number B18.028) and obtained after written informed consent of the donor.

2.2 | Specimen collection and processing

Human embryonic and fetal inner ears were collected after elective termination of pregnancy by vacuum aspiration. Embryonic or fetal age (in weeks, W), defined as the duration since fertilization, was determined by obstetric ultrasonography prior to termination, with a standard error of 2 days. Gestational age (GW), that is, the age of pregnancy taken from the beginning of the last menstrual period, is estimated by adding 2 weeks to either embryonic or fetal age. In contrast to previous studies from our group, we have decided to use embryonic and fetal age in this article, given the increasing number of publications using this nomenclature. Tissue was obtained at the following developmental stages: W5.0 ($n = 1$), W5.3 ($n = 1$), W7 ($n = 3$), W8 ($n = 3$), W9 ($n = 6$), W10 ($n = 3$), W10.4 ($n = 1$), W11, ($n = 3$), W12 ($n = 3$), W13 ($n = 2$), and W14 ($n = 3$). Time between termination and collection was kept to a minimum of several minutes. Inner ears were processed as previously described (Locher et al., 2013). Briefly, inner ears were harvested from vacuum-aspirated tissue collected in phosphate-buffered saline pH 7.4 (PBS), transferred to 4% formaldehyde (prepared from paraformaldehyde) in 0.1 M Na^+/K^+-phosphate buffer (pH 7.4), and fixed for at least one night at 4°C. Inner ears from W12 and older were decalcified for 1–3 weeks in 10% EDTA-2Na (Sigma-Aldrich, St. Louis, MO, USA) in distilled water (pH 7.4) at 4°C prior to dehydration in an ascending ethanol (70%–99%) series, clearing in xylene, and embedding in paraffin wax. Vestibular tissue from patients undergoing translabyrinthine vestibular schwannoma surgery was collected and processed similarly.

2.3 | Histology and immunohistochemistry

Sections (5 μm) were cut using a HM 355 S rotary microtome (Thermo Fisher Diagnostics B.V., Landsmeer, the Netherlands).

Sections were deparaffinized in xylene and rehydrated in a descending series of ethanol (96%–50%) and several rinses in deionized water. Every 10–20 sections, one section was selected for routine staining with hematoxylin and eosin (H&E).

Antigen unmasking was performed either in 10 mM sodium citrate buffer (pH 6.0) for 12 min at 97°C or by means of digestion with 20 μg/ml proteinase K in PBS for 5 min at room temperature, the latter in case of laminin immunostaining.

After rinsing in washing buffer (consisting of 0.05% Tween-20 [Promega, Madison, WI, USA]), sections were incubated for 30 min with blocking solution (consisting of 5% bovine serum albumin [BSA; Sigma-Aldrich, St. Louis, MO, USA] and 0.05% Tween-20 in PBS) followed by overnight incubation at 4°C with the following primary antibodies, appropriately diluted in blocking solution, either as single, double, or triple immunostainings: rabbit anti-Dct/Trp2 immunoglobulin (DCT, 1:40, Novus Cat# NBP1-86893, RRID:AB_11025576), mouse anti-ECAD immunoglobulin (1:20, BD Biosciences Cat# 610182, RRID:AB_397581), mouse anti-KIT immunoglobulin (1:200, Novus Cat# NBP2-34487), rabbit anti-KITLG immunoglobulin (1:100, Novus Cat# NBP2-67622), rabbit anti-Melan-A/MART-1 immunoglobulin (A19-P, 1:200, Novus Cat# NBP1-30151, RRID:AB_1987285), rabbit anti-MITF immunoglobulin (MITF, 1:100, Abnova Cat# PAB18189, RRID:AB_10713038), mouse anti-Na^+/K^+-ATPase α1 immunoglobulin (ATP1a1, 1:200, Novus Cat# NB300-146, RRID:AB_2060981), rabbit anti-laminin immunoglobulin (LAM, 1:100, Z009701, Dako, Santa Clara, CA, USA), mouse anti-PAX3 immunoglobulin (1:20, DSHB Cat# O13081), mouse anti-PCAD immunoglobulin (1:50, R and D Systems Cat# MAB861, RRID:AB_2077770), mouse anti-class III beta-tubulin immunoglobulin (TUBB3, 1:200, Abcam Cat# ab18207, RRID:AB_444319), and goat anti-SOX10 immunoglobulin (1:100, Thermo Fisher Scientific Cat# PA5-47001, RRID:AB_2608449). Next, sections were incubated at room temperature with the following Alexa Fluor®-conjugated secondary antibodies for 2 hr: AF488 donkey anti-rabbit immunoglobulin (Abcam Cat# ab150061, RRID:AB_2571722), AF488 donkey anti-goat immunoglobulin (Abcam Cat# ab150133, RRID:AB_2832252), AF594 donkey anti-mouse immunoglobulin (Thermo Fisher Scientific Cat# A-21203, RRID:AB_2535789), and AF680 donkey anti-rabbit immunoglobulin (Thermo Fisher Scientific Cat# A10043, RRID:AB_2534018), diluted at 1:500 in blocking solution. Nuclei were stained with 4′,6-diamidino-2-phenylindole (DAPI; 1:1,000, Vector Laboratories Ltd., Peterborough, UK). Sections were mounted with ProLong™ Gold Antifade Mountant (Thermo Fisher Scientific, Waltham, MA, USA). Negative controls were carried out by matching isotype controls and omitting primary antibodies. Positive controls were carried out by staining sections of known positive human tissue samples based upon their protein expression profiles. At least three separate immunostaining experiments were performed with each primary antibody.

2.4 | Image acquisition and processing

Sections stained with H&E were digitized using a Pannoramic MIDI scanner and viewed with CaseViewer software (3DHISTECH, Budapest, Hungary). Pseudocolor images of immunostained sections were acquired with a Leica SP8 confocal laser scanning microscope using Leica objectives (20×/0.7 dry HC PL Apo, 40×/1.3 oil HC PL Apo CS2, 63×/1.4 oil HC PL Apo or 100×/1.3 oil HC PL Fluotar), operating under Leica Application Suite X microscope software (LAS X, Leica Microsystems, Buffalo Grove, IL, USA). Obtained images were optimized using Huygens Deconvolution software (Scientific Volume Imaging, Hilversum, the Netherlands). Maximal projections were obtained from image stacks with optimized z-step size. Brightness and contrast adjustments were performed with Fiji (ImageJ version 1.52p) or Adobe Photoshop CC 2018. For separate channels, the corresponding author can be contacted.

3 | RESULTS

3.1 | Melanoblasts are located between the otic vesicle and the glossopharyngeal nerve at W5

In order to determine the origin of vestibular melanocytes, we studied the presence of melanoblasts in the human embryo at W5. We first stained for the melanoblast markers DCT and MITF. Both DCT and MITF antibodies appeared to selectively immunostain the mitotic cells surrounding the otic vesicle and lining the lumen of both the otic vesicle and neural tube (Figure S1). Based on this unexpected expression pattern, we hypothesized that DCT and MITF immunostain targets other than the melanoblasts at this developmental stage. Next, we included additional melanocyte lineage markers SOX10, PAX3, and MLANA. SOX10 is expressed by (progenitor) glial cells and melanoblasts/melanocytes, whereas PAX3 and MLANA are specifically expressed in the melanocytic lineage. To visualize general morphology, we performed staining with H&E (Figure 2A,B) and immunostaining for class III beta-tubulin (TUBB3; Figure 2C), indicative for various neural and epithelial cells. $SOX10^+$ cells were seen around the peripheral projections and ganglia of the developing facial and glossopharyngeal nerves. In addition, $SOX10^+$ cells were also located between the otic vesicle and the glossopharyngeal nerve (Figure 2D,D″). However, only these $SOX10^+$ cells expressed both PAX3 and MLANA, hence identifying them as melanoblasts/melanocytes rather than glial cells (Figure 2D-D′′′). No $SOX10^+PAX3^+MLANA^+$ cells were seen cranially from the otic vesicle or surrounding the facio-acoustic ganglion complex (data not shown). Together, our findings show presence of a $SOX10^+PAX3^+MLANA^+$ melanoblast/melanocyte progenitor population between the developing otic vesicle and the peripheral projection of the glossopharyngeal nerve.

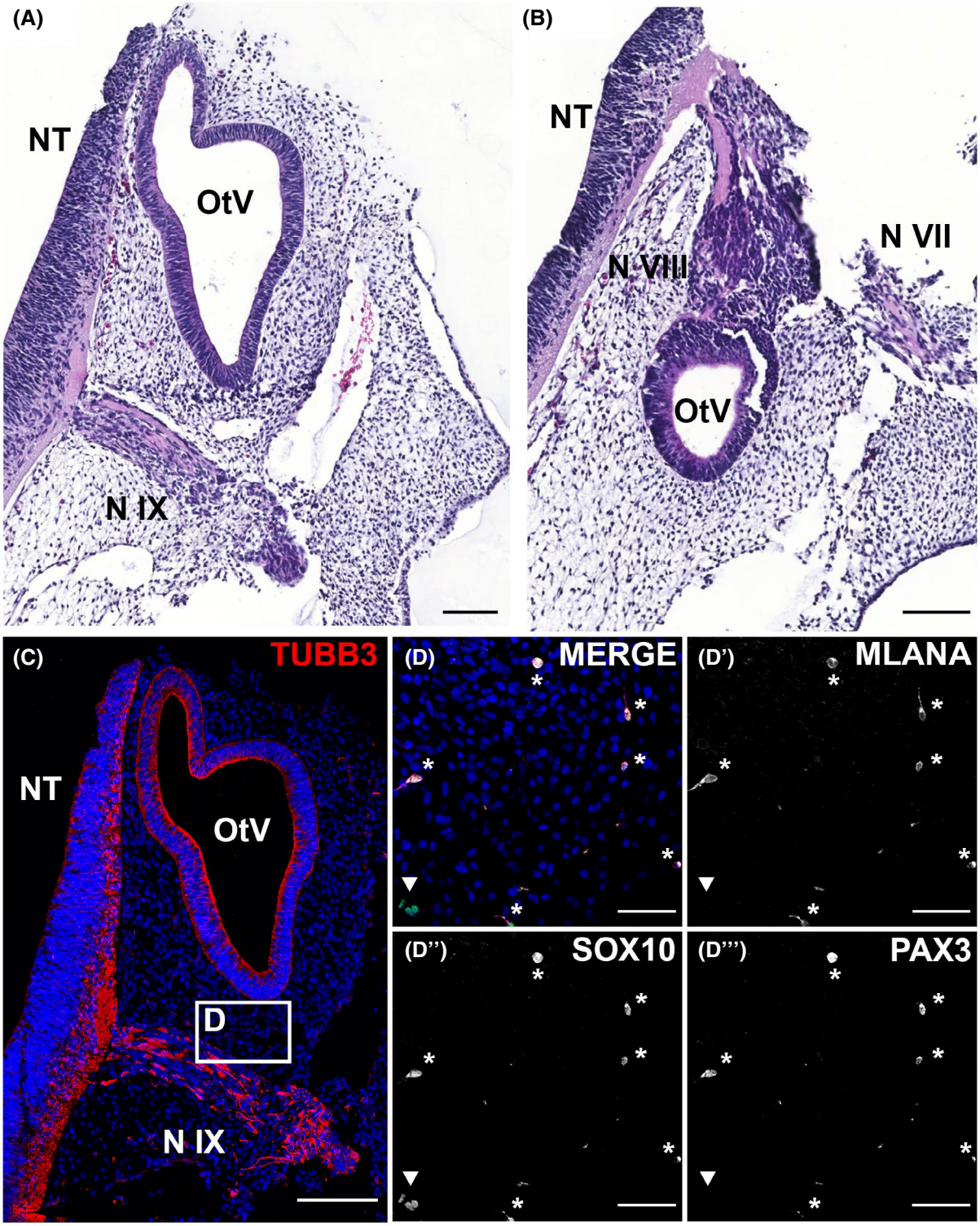


FIGURE 2 Melanoblasts between the otic vesicle and the glossopharyngeal nerve at W5 of development. (A) H&E overview showing the otic vesicle (OtV), the neural tube (NT), and the glossopharyngeal nerve and ganglion (N IX). (B) H&E overview showing the OtV, the NT, and the facio-acoustic ganglion complex and projections of the facial (N VII) and vestibulocochlear nerves (N VIII). (C) Overview of the OtV, the NT, and the projection and ganglion of the glossopharyngeal nerve (N IX), immunostained with class III beta-tubulin. (D-D‴) Detail of C: $SOX10^{+}PAX3^{+}MLANA^{+}$ melanoblasts are scattered throughout the area between the otic vesicle and the projection of the glossopharyngeal nerve (indicated with asterisks). Schwann cell precursors, which are $SOX10^{+}PAX3^{-}MLANA^{-}$, are seen in the projection and ganglion of the glossopharyngeal nerve (indicated with a triangle). Green: SOX10 (D‴); red: TUBB3 (C), PAX3 (D‴); and magenta: MLANA (D'). Scale bars: 200 μm (A-C) and 50 μm (D-D‴)

3.2 | Vestibular melanocytes are seen around the vestibular organs at W7

At W7, spindle-shaped MLANA$^+$ melanocytes with short dendritic processes (Figure 3H) were present directly under the extramacular epithelia of the utricle and ampullae and in the future periotic mesenchyme (Figure 3A-C,F,G), but not surrounding or lying underneath the extramacular epithelia of the saccule (not shown). Also, MLANA$^+$ melanocytes were present in the future periotic mesenchyme surrounding the semicircular canals ([SCC], Figure 3D-E). Cells in the future periotic mesenchyme or the epithelial cells in the utricle (Figure 3F), SCC (Figure 3E), saccule, or ampullae (data not shown) did not express Na^+/K^+-ATPase α1, a transmembrane ion pump which is strongly expressed by dark cells in the adult rat vestibular system and to a lesser extent by the vestibular sensory cells (Cate et al., 1994; Schuth et al., 2014). In addition, at this stage immunostaining of PAX3 was absent in melanocytes, indicating they had developed into a more mature phenotype (data not shown).

3.3 | Between W8 and W10, vestibular melanocytes are located in the transitional zone and dark cell area

At W8, the number of melanocytes increased around the utricular wall (Figure 4A,B), near the transitional zone of the ampullae (the peripheral layer of non-sensory epithelial cells separating the vestibular sensory cells from the dark cells [Figure 4C,D,G]) and in the periotic mesenchyme (Figure 4E,F), whereas melanocytes could not be seen near the saccule (data not shown). Several melanocytes were seen in close proximity of the transitional zone of the ampullae (Figure 4G). Strong staining for Na^+/K^+-ATPase α1 was seen in the basolateral and apical membranes of the sensory cells in the utricle and ampulla. The transitional zone of the utricle and ampullae, the periotic mesenchyme surrounding the vestibular organs and the single epithelium were also found to express Na^+/K^+-ATPase α1, although less intense than the sensory epithelium (Figure 4B,D,F,G).

At W9, some melanocytes showed close contact with epithelial cells near the developing dark cell areas (Figure 5D,G-J). A number of melanocytes were seen under the epithelium of the crista neglecta, a rudimentary structure believed to go into regression at later stages, whereas at this time none were seen in the dark cell area directly adjacent to the crista neglecta (Figure 5E,F). Melanocytes could also not be observed around the saccular epithelium and associated saccular periotic mesenchyme (Figure 5A,C). Strong immunostaining for Na^+/K^+-ATPase α1 was present in both the apical and basolateral membranes of the sensory epithelium of saccule, utricle, and ampullae. In addition, it was highly expressed by the basolateral membranes of the dark cell epithelium located laterally to the ampullae, between the utricle and the ampulla as well as in the utricular roof opposite to the macula (Figure 5B-D,F-J). Less intense immunostaining was seen in the transitional zone and the periotic mesenchyme. No immunostaining for Na^+/K^+-ATPase α1 was seen in the epithelial cells of the crista neglecta, while expression was found in the basolateral membranes of the adjacent dark cell epithelium (Figure 5E-F).

At W10, melanocytes were observed underneath the epithelium of the dark cell area located laterally to the ampullae, in the utricular roof opposite the utricular macula and in the epithelial folds between the utricle and ampullae (Figure 6A,C-G). Melanocytes were also observed in the epithelial fold separating the opening of the endolymphatic duct and the shared lumen of the utricle and saccule (Figure 6B). Expression of Na^+/K^+-ATPase α1 became gradually more intense in the dark cell epithelium and in both sensory and transitional cells (Figure 6C-G).

3.4 | Between W10 and W11, the number of vestibular melanocytes in the dark cell area increases rapidly

During W10, the number of vestibular melanocytes underlying the transitional zones of the ampullae and utricle as well as the dark cell epithelium located laterally to these, increased rapidly (Figure 7A,C,D). Dendritic processes of the melanocytes were seen reaching out toward the apical surface of the epithelium, whereas only a few melanocytes were seen in the periotic mesenchyme at this stage (Figure 7A,B). The basement membrane protein laminin was continuous in areas without melanocytes (Figure 7B). In contract, at the sites where melanocytes were clustering and made contact with the epithelial cells, laminin was irregularly stained indicating that the dendritic processes of the melanocytes penetrated the basement membrane (Figure 7B). Expression of Na^+/K^+-ATPase α1 appeared slightly reduced in the sensory and transitional cells as well as in the periotic mesenchyme when compared to previous weeks. It had become more spatially confined in the dark cell epithelium in the utricular roof opposite the macula, in the epithelial folds separating ampullae and utricle and in the dark cell epithelium laterally to the ampulla (Figure 7A,C).

3.5 | At W11, vestibular melanocytes are aligned with dark cell epithelium

At W11, no vestibular melanocytes were observed in the periotic mesenchyme surrounding the ampullae, the utricular wall, the utricular roof opposite the macula, or surrounding the utricular and saccular maculae (Figure 8A). Melanocytes were closely associated with the dark cell epithelium laterally to the ampullae (Figure 8A), near to the utricular transitional zone (Figure 8B), opposite to the utricle in epithelial

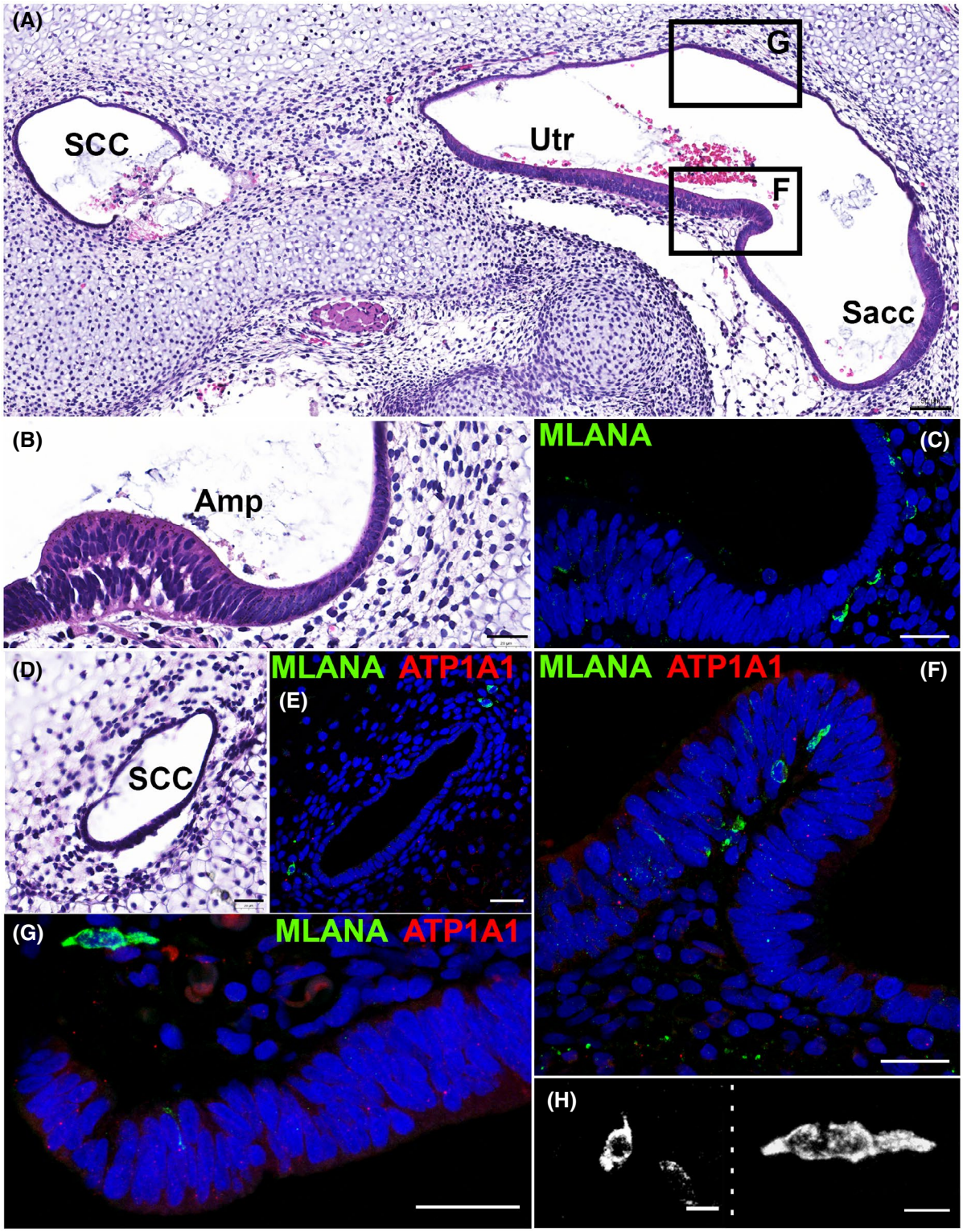


FIGURE 3 Melanocytes located around the vestibular organs at W7 of development. (A) H&E overview showing a transected semicircular canal (SCC), the utricle (Utr), and the saccule (Sacc). (B) H&E overview of an ampulla (Amp). (C) Melanocytes stained with MLANA underneath the transitional epithelium of the ampulla. (D) H&E overview of a transection of an SCC. (E) Melanocytes in the future periotic mesenchyme surrounding the SCC. (F) Detail of A: melanocytes within an epithelial fold near the utricular macula. (G) Detail of A: melanocyte underneath the dark cell epithelium in the utricular roof opposite to the macula. (H) Higher magnifications of melanocytes from panels E and G, showing short dendritic processes and their spindle-shaped morphology. No expression of Na^+/K^+-ATPase α1 was observed (E, F, and G). Green: MLANA; red: ATP1A1; and blue: DAPI. Scale bars: 5 μm (H), 20 μm (B, C, D, E, F, and G), and 50 μm (A)

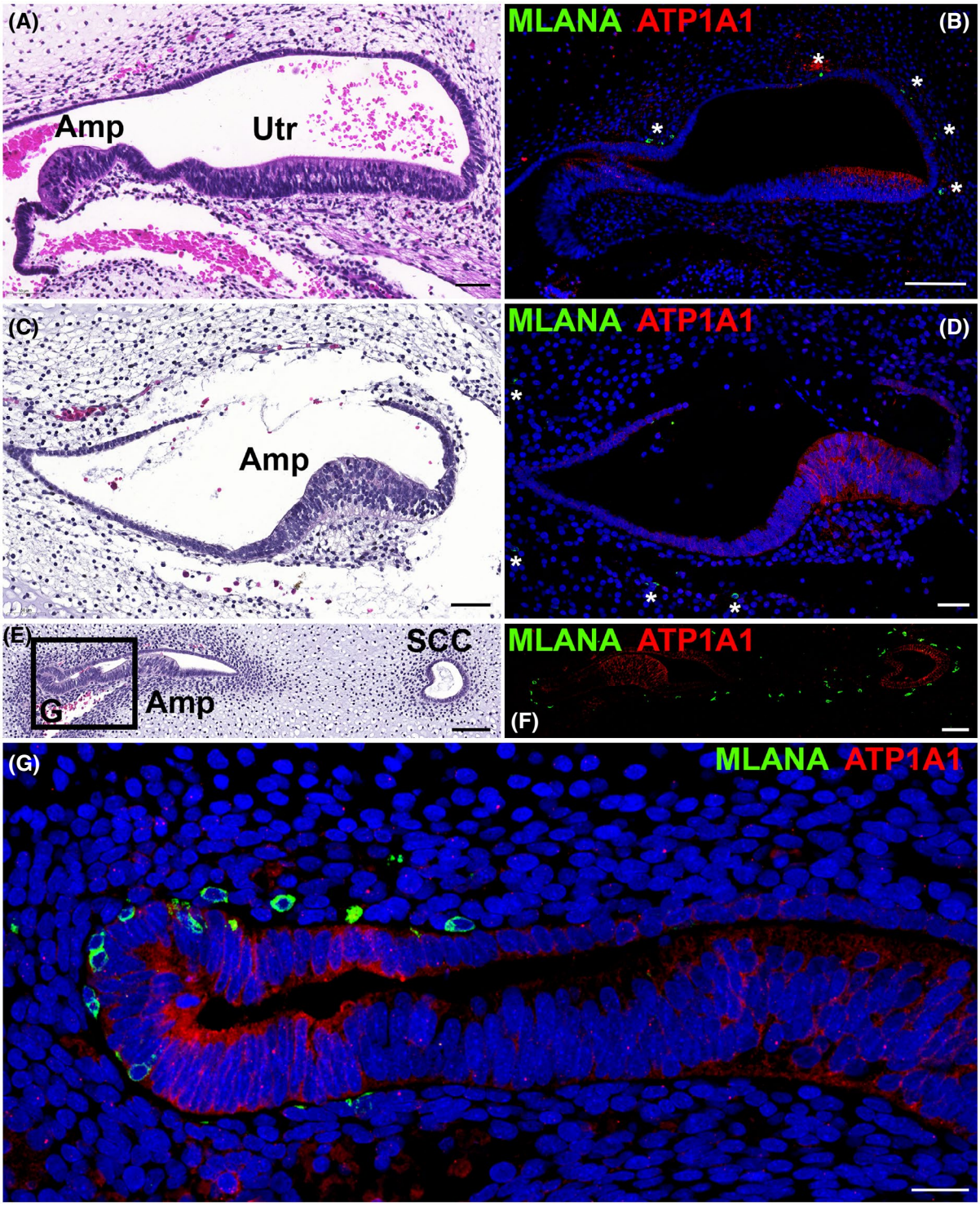


FIGURE 4 Utricle and ampullae at W8 of development. (A) H&E overview of the vestibular organs at W8, showing transections of an ampulla (Amp) and the utricle (Utr). (B) Melanocytes (asterisks) migrating through the periotic mesenchyme surrounding the ampulla and the utricle. (C) H&E overview of an ampulla. (D) Ampulla with melanocytes in the periotic mesenchyme (asterisk) and strong expression of Na^+/K^+-ATPase α1. (E) H&E overview of an ampulla and a transected semicircular canal (SCC). (F) Melanocytes migrating through the periotic mesenchyme surrounding the ampulla and SCC. (G) Detail of E: transitional zone adjacent to the ampullar crista containing melanocytes underneath the epithelium expressing Na^+/K^+-ATPase α1. Green: MLANA; red: ATP1A1; and blue: DAPI. Scale bars: 20 μm (F), 50 μm (A, C), and 100 μm (B, D, E, and F)

folds (Figure 8C), but not underneath the saccular epithelia (Figure 8E). Compared to W10, laminin showed a more irregular staining pattern below the dark cell epithelium between utricle and ampulla (Figure 8F) and in the epithelial folds opposite to the utricle (Figure 8D). A clear distinction between interrupted and intact (not interrupted) basement

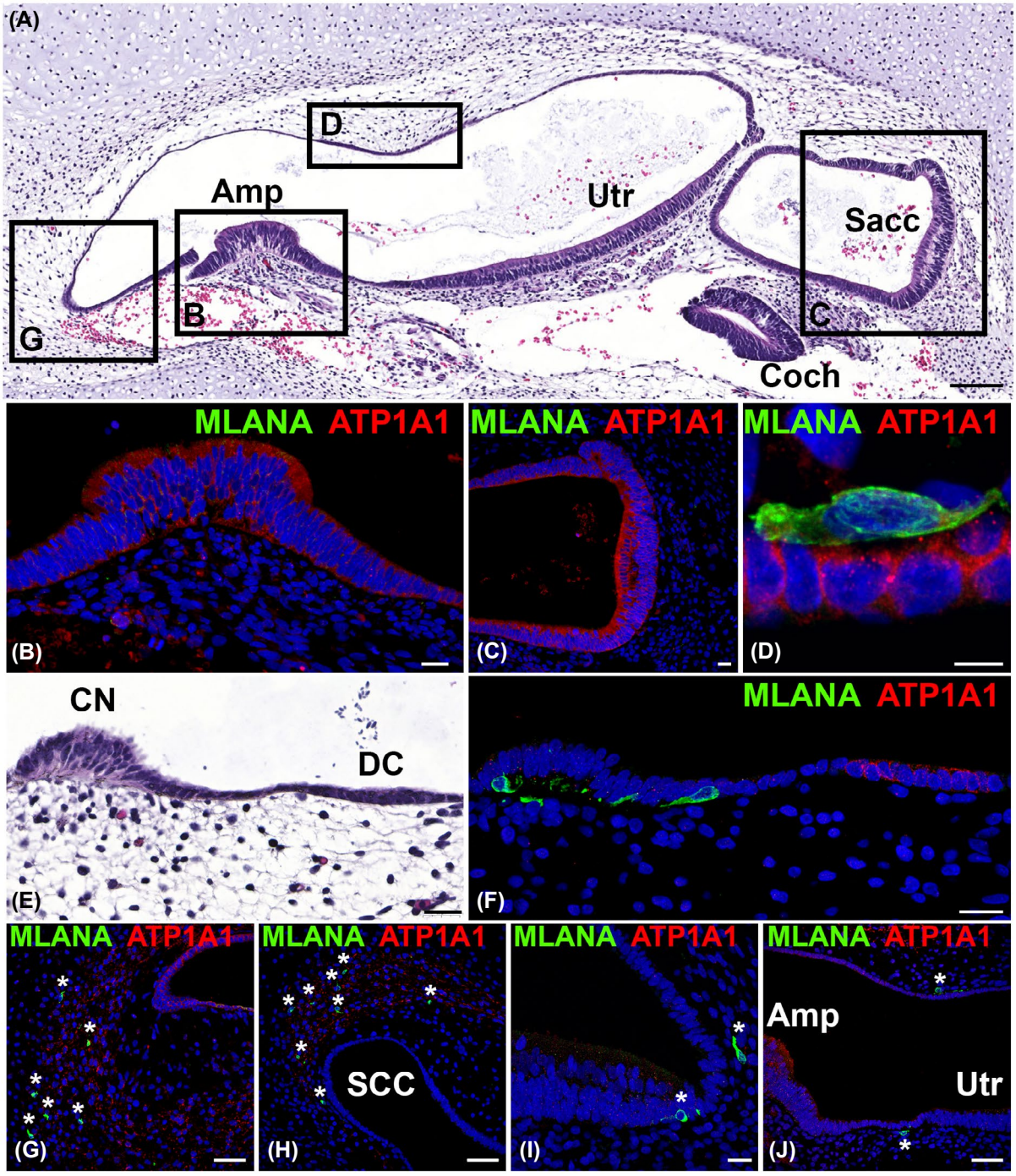


FIGURE 5 Utricle, saccule, and ampullae at W9 of development. (A) H&E overview of ampulla (Amp), utricle (Utr), saccule (Sacc), and cochlear duct (Coch). (B) Detail of A: ampulla showing cells expressing Na^+/K^+-ATPase α1, but lacking melanocytes. (C) Detail of A: no melanocytes were found surrounding the saccule. (D) Detail of A: melanocyte underneath the dark cell epithelium opposite the ampullar crista. (E) H&E staining of the crista neglecta (CN) and dark cell epithelium (DC). (F) Melanocytes are lying underneath the crista neglecta, but are absent under the dark cell epithelium. (G) Detail of A: Melanocytes (asterisks) in the periotic mesenchyme surrounding the ampulla. (H) Melanocytes (asterisks) in the periotic mesenchyme surrounding the semicircular canal (SCC). (I) Melanocytes (asterisks) near the transitional zone in the utricle. (J) Melanocytes (asterisks) underneath the dark cell area in the utricular roof opposite the macula and in between the ampulla and utricle. Green: MLANA; red: ATP1A1; and blue: DAPI. Scale bars: 5 μm (D), 20 μm (B, C, E, F, and I), 50 μm (G, H, and J), and 100 μm (A)

membranes could be made between epithelium with melanocytes and single epithelium without melanocytes. The dark cell epithelium demonstrated a strong immunostaining for Na^+/K^+-ATPase α1, while its expression in the sensory epithelium of the ampullae, utricle, and saccule was present, but stained less intense as compared to the dark cells

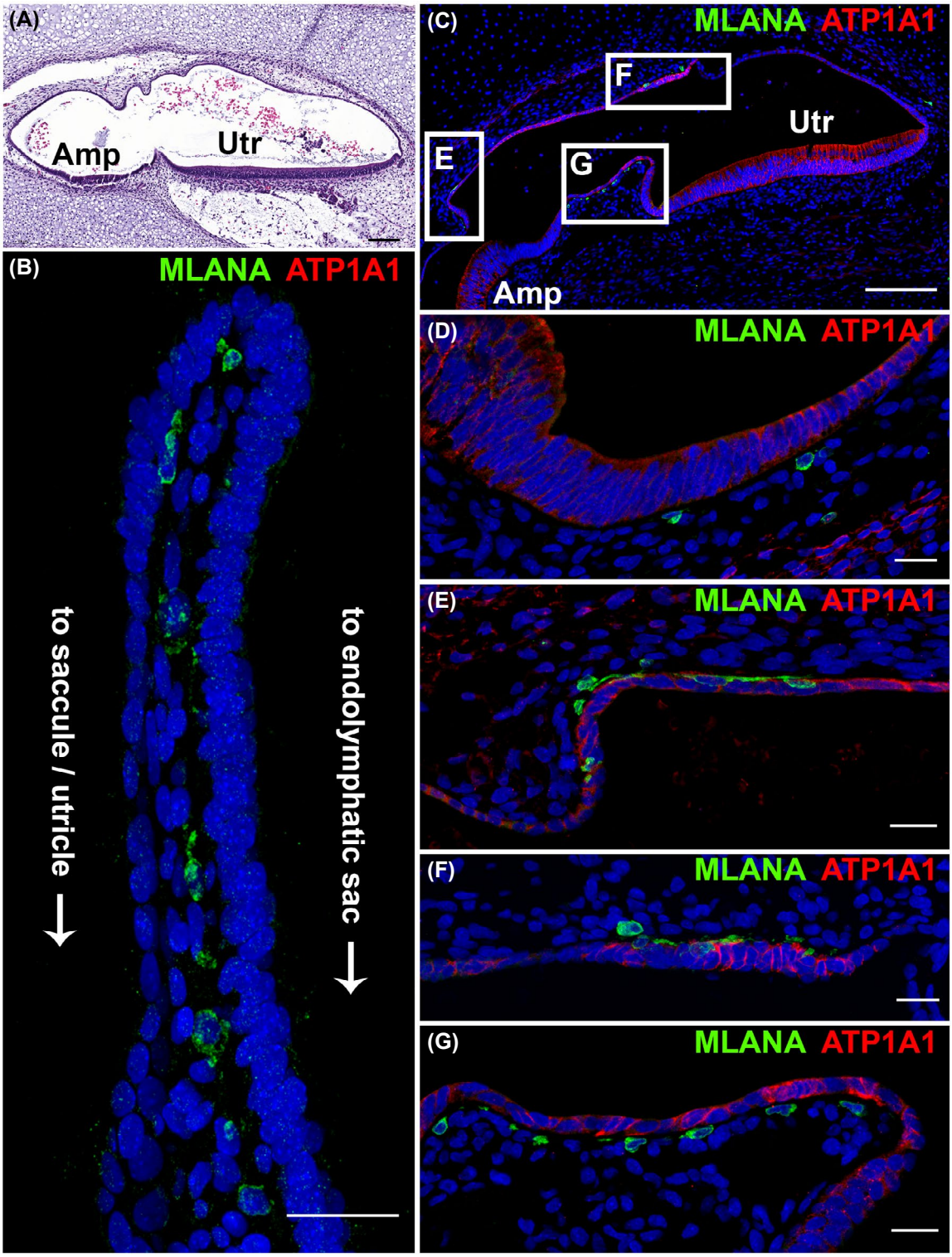


FIGURE 6 Utricle and ampullae at W10 of development. (A) H&E overview of ampulla (Amp) and utricle (Utr). (B) Melanocytes migrating through an epithelial fold separating the endolymphatic duct and the common lumen of the utricle and saccule. (C) Overview of ampulla and utricle. (D) A small number of melanocytes underlying the ampullar transitional zone. (E) Detail of C: melanocytes underneath the dark cell epithelium opposite to the ampullar crista. (F) Detail of C: melanocytes underneath the dark cell epithelium opposite the utricular macula. (G) Detail of C: melanocytes in between the ampulla and utricle. Green: MLANA; red: ATP1A1; and blue: DAPI. Scale bars: 20 μm (B, C, D, E, F, and G) and 100 μm (A)

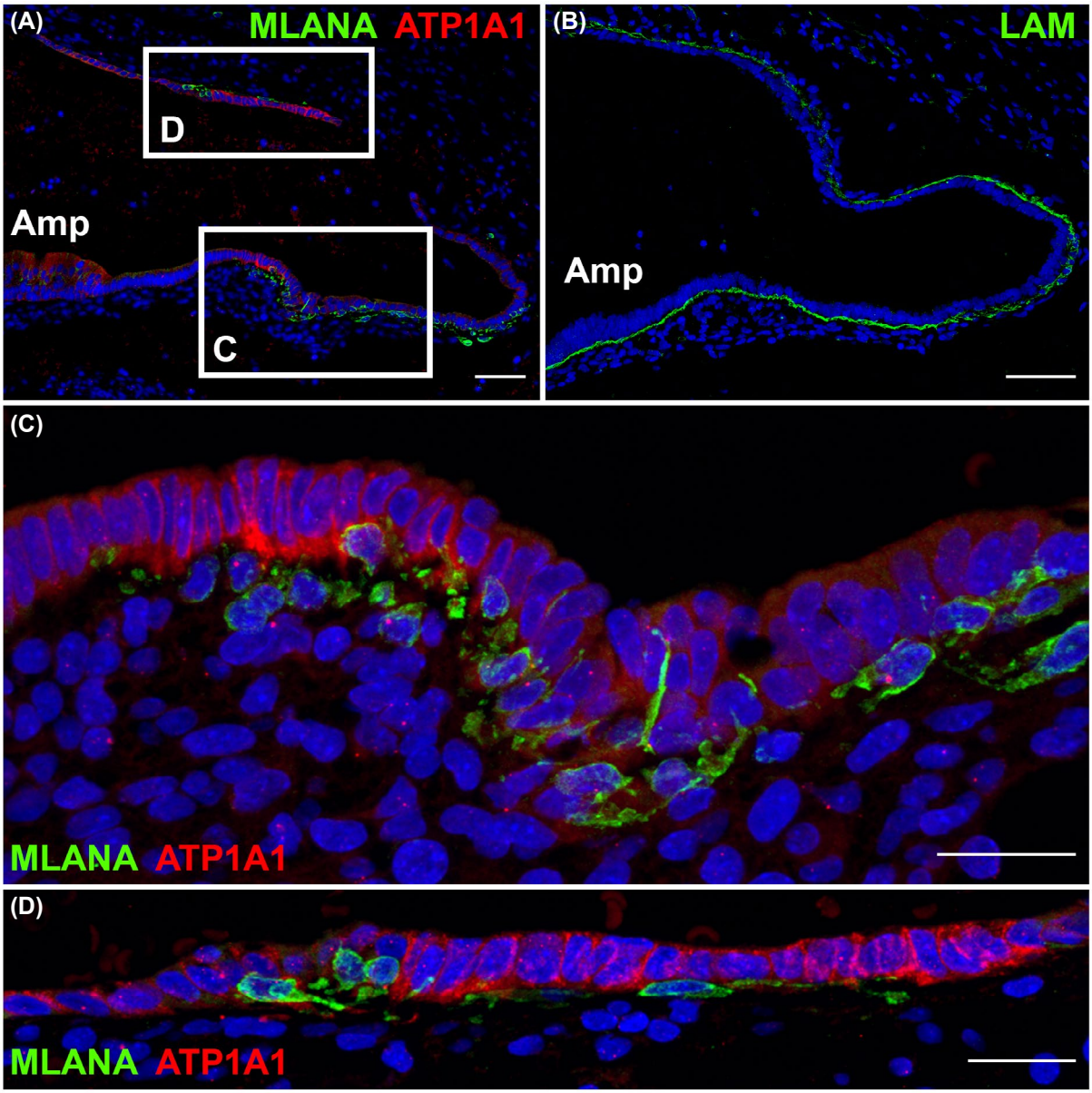


FIGURE 7 Utricle and ampullae at W10.4 of development. (A) Overview of ampulla, transitional zone, and dark cell epithelium. (B) Basement membrane protein laminin stains irregularly at sites where melanocytes group underneath the dark cell epithelium. (C) Detail of A: melanocytes are associated with the transitional cells and dark cells. Note the dendritic processes reaching toward the apical regions of the epithelium. (D) Detail of A: dark cell epithelium in the roof of the ampulla opposite of the crista. Green: MLANA (A, C and D) or laminin (B); red: ATP1A1; and blue: DAPI. Scale bars: 20 μm (C and D) and 50 μm (A and B)

(Figure 8A,B,E). At this point, the transitional zones of the ampulla and utricle were less intensely stained as compared to the dark cells (Figure 8B).

3.6 | During W12 and W13, Na^+/K^+-ATPase α1 is further confined to the dark cell area

During the next 2 weeks, no evident changes occurred in the number or location of vestibular melanocytes (Figures S2 and S3). Expression of Na^+/K^+-ATPase α1 was restricted to the basolateral membranes of the dark cell epithelium located laterally to the ampullae, between the ampullae and utricle, and in the epithelial folds of the utricle. The sensory epithelium and transitional zone showed a weaker expression of Na^+/K^+-ATPase α1 as compared to the dark cells.

3.7 | At W14, the dark cell area shows a mature profile

At W14, melanocytes formed a dense network lining the dark cell epithelium and Na^+/K^+-ATPase α1 became further confined to the basolateral membranes of the dark cells

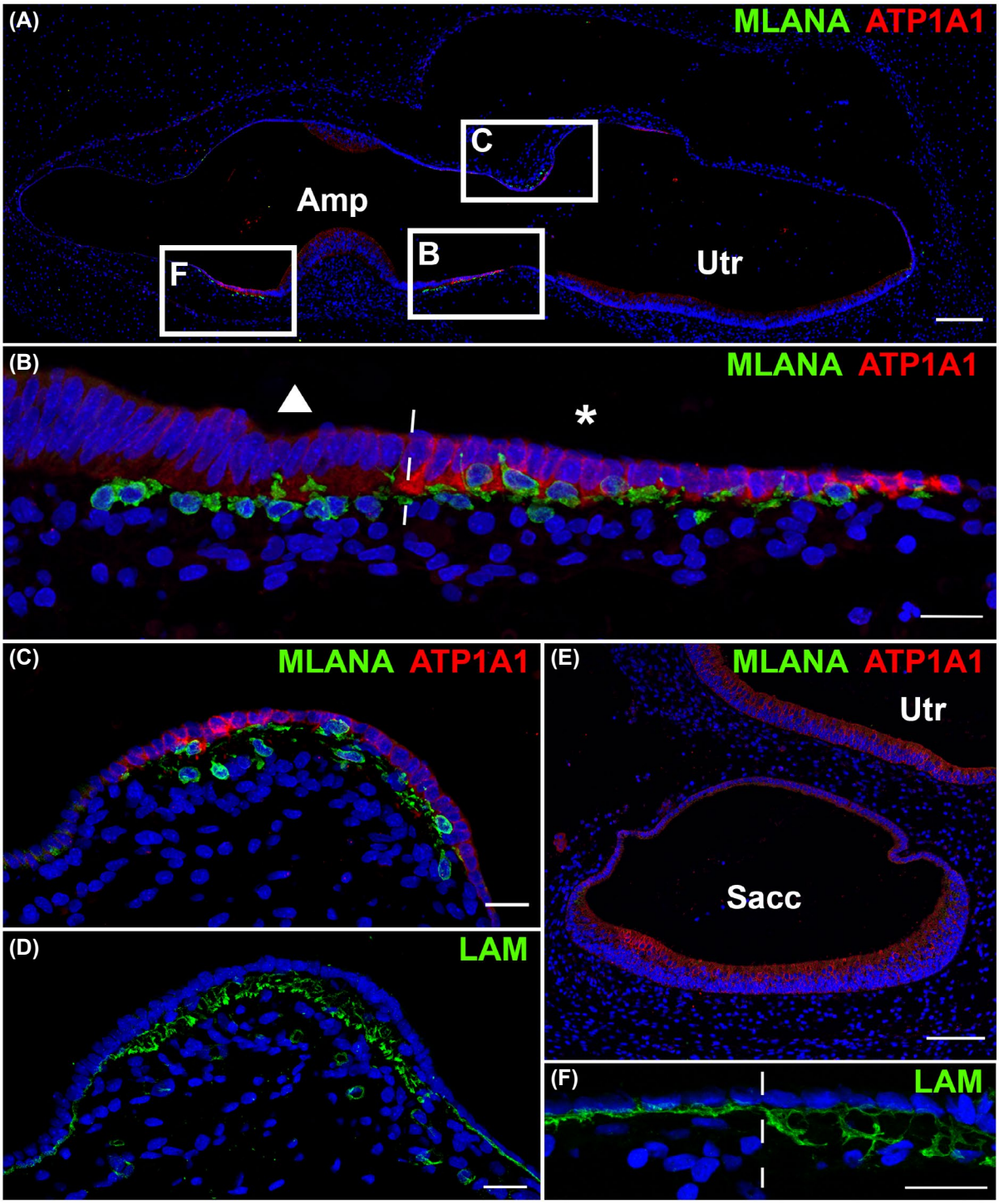


FIGURE 8 Utricle, ampulla, and saccule at W11 of development. (A) Overview of utricle (Utr) and ampulla (Amp). (B) Detail of A: transitional zone and dark cell epithelium with underlying melanocytes. Triangle indicator shows an area with less intense immunostaining of Na^+/K^+-ATPase α1 as compared to the area indicated with an asterisk. (C) Detail of A: showing an epithelial fold with dark cell epithelium. (D) Detail of A: showing irregular, interrupted laminin staining pattern of the basement membrane at the site where melanocytes are positioned underneath the epithelium. (E) Absence of melanocytes near the saccule (Sacc). Note the intermediate immunostaining of Na^+/K^+-ATPase α1 in the utricular and saccular maculae. (F) Intact (left) versus interrupted (right) basement membrane, showing the impact of melanocytes associated with the dark cells. Green: MLANA (A–C and E) or laminin (D and F); red: ATP1A1; and blue: DAPI. Scale bars: 20 μm (B, C, D, E, and F) and 100 μm (A)

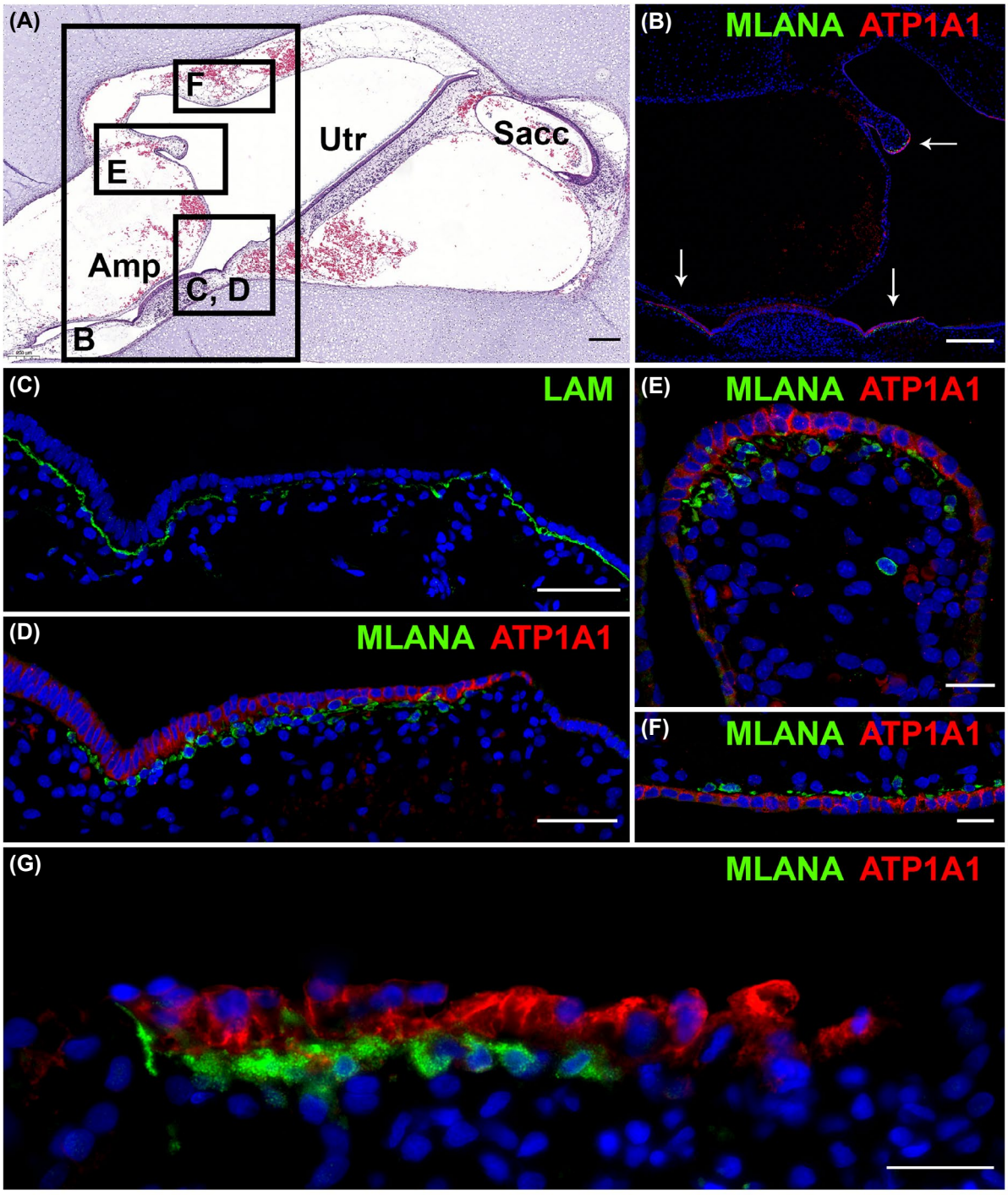


FIGURE 9 Utricle and ampulla at W14 of development and adult ampulla. (A) H&E overview of utricle (Utr), ampulla (Amp), and saccule (Sacc). (B) Detail of A: showing ampulla and epithelial fold with dark cell epithelium (arrows). (C) Irregular laminin staining profile of the basement membrane of the transitional zone and dark cell epithelium near the ampulla. (D) Consecutive immunostained section with melanocytes underlying the transitional zone and dark cell epithelium near the ampulla. (E) Detail of A: showing the epithelial fold containing dark cell epithelium with subepithelial connective tissue. (F) Detail of A: showing the dark cell epithelium in the utricular roof. (G) Dark cell area of an adult ampulla. Green: MLANA (B and D–G) or laminin (C); red: ATP1A1; and blue: DAPI. Scale bars: 20 μm (E, F and G), 50 μm (C and D), and 200 μm (A and B)

(Figure 9A,B,D–F). The sensory domain and transitional zones continued to express Na^+/K^+-ATPase α1, although to a lesser degree than the dark cells, which became increasingly more evident. The staining pattern of laminin was more diffuse underneath the dark cell epithelium, compared to the preceding weeks (Figure 9C). At this stage, the dark cell area showed a mature profile similar to the ampullar dark cell area collected from an adult patient (Figure 9G).

3.8 | Inner ear melanocytes temporally express cadherins involved in migration

Cadherins are known to mediate interaction between the micro-environment and migrating neural crest cells along the dorso-lateral and ventral pathways (for a review, see Pla et al., 2001). In mice, expression of E- and P-cadherin (ECAD and PCAD) are closely associated with the distinct stages of melanoblast migration and maturation in the skin (Nishimura et al., 1999). In order to correlate our static observations with the complex dynamics of melanoblast migration, we immunostained for ECAD and PCAD. At W5, both ECAD and PCAD were specifically expressed by the entire otic vesicle epithelium (data not shown) and by the $SOX10^+$ melanoblasts located caudally from the otic vesicle (Figure 10A-A′,B-B′), but not by $SOX10^+$ glial (progenitor) cells (data not shown). At W9 and W10, the transitional and dark cell epithelia strongly stained for both cadherins, whereas the sensory domain stained less intensely (Figure 10C-F). $ECAD^+$ melanocytes were seen underneath the transitional cells (Figure 10E-E′) and the dark cells (Figure 10G-G′). Melanocytes also faintly immunostained for PCAD, and where they made contact with epithelial cells, a punctated pattern was visible (Figure 10F-F′; see asterisks in Figure 10H-H′). At W14, no immunostaining for ECAD was seen in the sensory domain, whereas transitional cells, dark cells and melanocytes showed strong expression of ECAD (Figure 10I-I″). In contrast, no $PCAD^+$ epithelial cells or melanocytes were seen at this stage (Figure 10J-J″). In summary, ECAD expression by otic melanocytes was seen at all investigated stages, whereas PCAD expression was gradually downregulated in these cells. The undifferentiated otic epithelium co-expressed both cadherins, but where PCAD was downregulated in all epithelial cells, ECAD expression became restricted to the transitional and dark cells.

3.9 | KIT and KIT ligand are expressed by melanocytes and dark cell epithelia, respectively

In mice, the interaction between KIT and its ligand KITLG plays a significant role in migration, survival, and proliferation of epidermal melanocytes (for a review, see Wehrle-Haller, 2003; Yoshida et al., 2001). To investigate a possible role of the KIT/KITLG axis in migration and guiding of inner ear melanocytes, we immunostained for both these proteins as well. At W9, no evident expression of KIT was seen in melanocytes (Figure 11A-A′). At W10 and W12, KIT^+ melanocytes were observed underneath the transitional and dark cell epithelia (Figure 11B,C). At W14, no KIT immunostaining was seen any longer in the melanocytes which at this stage resided exclusively underneath the dark cells (Figure 11D-D′). Regarding KITLG, at W9 only a punctated pattern was seen in the sensory domain of the ampulla (Figure 11E). At W10, expression of KITLG became more intense, and was visible as membranous immunostaining in the dark cell epithelium and as a punctated pattern in the subepithelial mesenchyme (Figure 11F-F′). At W12, dark cell epithelia showed a strong punctated pattern and membranous immunostaining (Figure 11G-G′), whereas at W14, only membranous immunostaining was visible in the dark cells epithelia (Figure 11H-H′). From W12 and onwards, hair cells and nerve fibers also stained for KITLG (data not shown).

4 | DISCUSSION

4.1 | On the origin of inner ear melanocytes

This is the first study to describe the developmental distribution of melanocytes in the human vestibular organs. The exact developmental origin of inner ear melanocytes has yet to be established. Both Schwann cells (the peripheral glial cell) and melanocytes are derived from multipotent neural crest cells, and can share a bipotent progenitor. However, both cell types can also arise from different neural crest origins and Schwann cell precursors can even transdifferentiate into the melanocytic lineage, making studies into the development of these cell types increasingly more complex (reviewed in Etchevers et al., 2019). In the cranial neural crest, both primary neural crest-derived cells and Schwann cell precursors migrating together with outgrowing nerves, have been shown to give rise to cranial melanocytes (Adameyko et al., 2009, 2012; Furlan & Adameyko, 2018). As the inner ear is a cranial structure (derived from the otic placode) one may hypothesize that its developmental population of both melanocytes and Schwann cells arise from one neural crest origin, especially since these two cell types are so intimately related. Inner ear Schwann cells are known to derive from neural crest cells emigrating at the level of rhombomere 4 where they migrate into the facio-acoustic ganglion complex and subsequently populate the spiral ganglion, Scarpa's ganglion and their nerve fibers during later developmental stages (D'Amico-Martel & Noden, 1983; Locher et al., 2014; Sandell et al., 2014). However, we have not observed any melanocytes at these locations in the human inner ear of W7, whereas we did find them migrating through the cochlear part of the otic capsule at W7 (Locher et al., 2015). This could be indicative of a different embryonic origin of these cell types in the inner ear. In order to further determine the origin of inner ear melanocytes, we have also studied human inner ear specimens of W5. At this stage the otic vesicle is differentiating into a vestibular and cochlear part, and spiral ganglion neurons have just delaminated

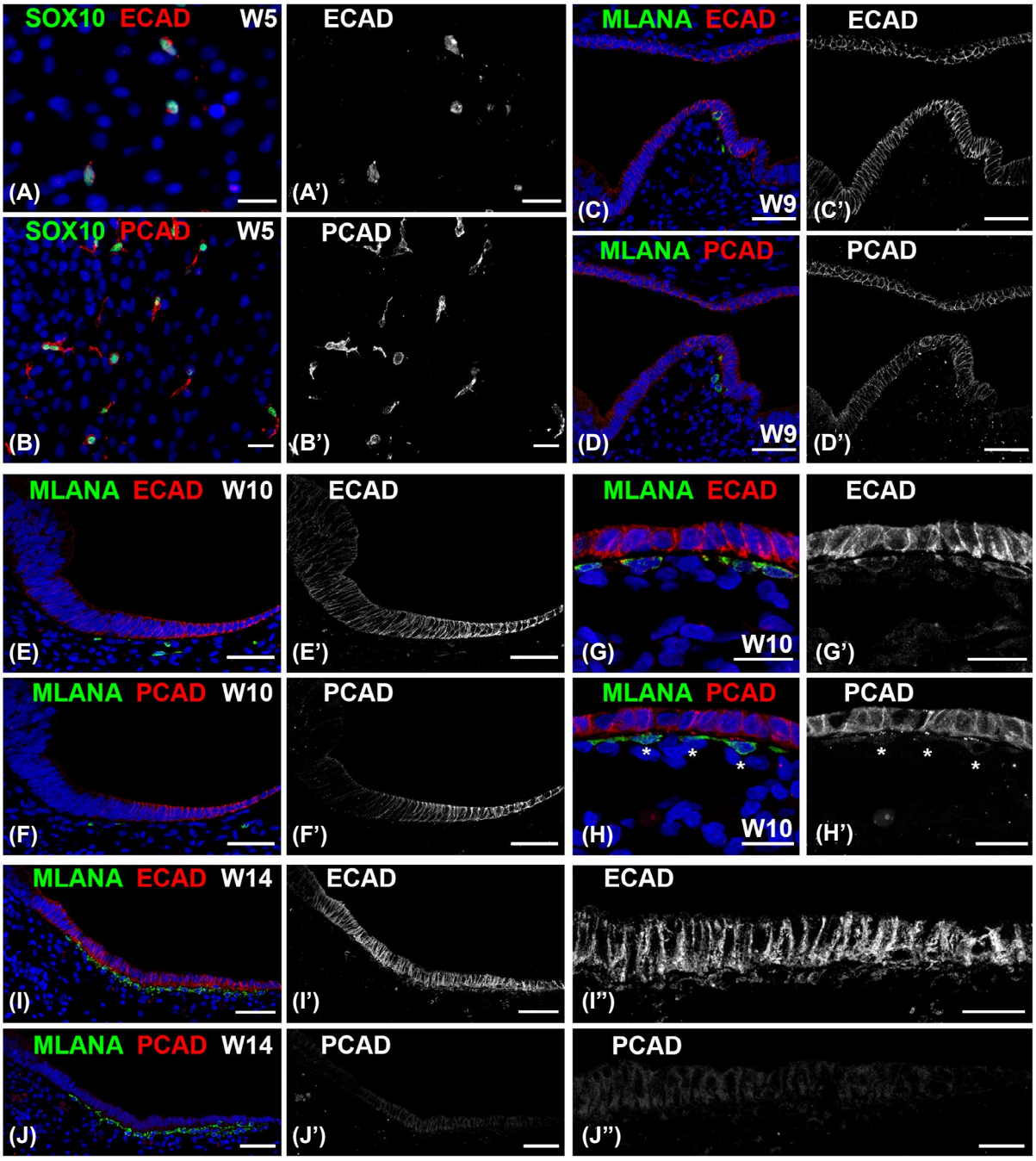


FIGURE 10 Melanoblasts dynamically express migration-related cadherins. (A-A′) At W5, SOX10$^+$ECAD$^+$ melanoblasts are seen between the otic vesicle and the glossopharyngeal nerve. (B-B′) At W5, SOX10$^+$ melanoblasts also immunostain for PCAD. (C-C′) ECAD$^+$ vestibular epithelia between utricle and ampulla. (D-D′) PCAD$^+$ vestibular epithelia between utricle and ampulla. (E-E′) At W10, ampullar transitional and dark cells immunostain for ECAD, whereas the sensory domain is less intense. Melanocytes faintly express ECAD. (F-F′) At W10, PCAD immunostaining is seen in the transitional and dark cell epithelia and faintly in subepithelial melanocytes. (G-G′) Dark cell epithelia and melanocytes express ECAD at W10. (H-H′) Dark cell epithelia and melanocytes express PCAD at W10. Note the punctated pattern of PCAD expression (see asterisks) where melanocytes make contact with epithelial cells. (I-I″) Dark cells and melanocytes express ECAD at W14. (J-J″) No PCAD expression is seen at W14. Green: SOX10 (A–B), MLANA (C–J); red: ECAD (A, C, E, G, and I), PCAD (B, D, F, H, and J); and blue: DAPI. Scale bars: 20 μm (A–B, G–H, I″ and J″) and 50 μm (C–E, I-I′ and J-J′)

from the otic epithelium. Immunostaining for melanocyte lineage-specific markers DCT and MITF, which are already expressed in the early melanocytic lineage at the melanoblasts stage (Opdecamp et al., 1997), stained various cells in the mesenchyme surrounding the otic vesicle, in the central projections of the glossopharyngeal nerve and in or around the vestibulocochlear ganglion. Strikingly, immunopositive cells were even observed lining the lumen

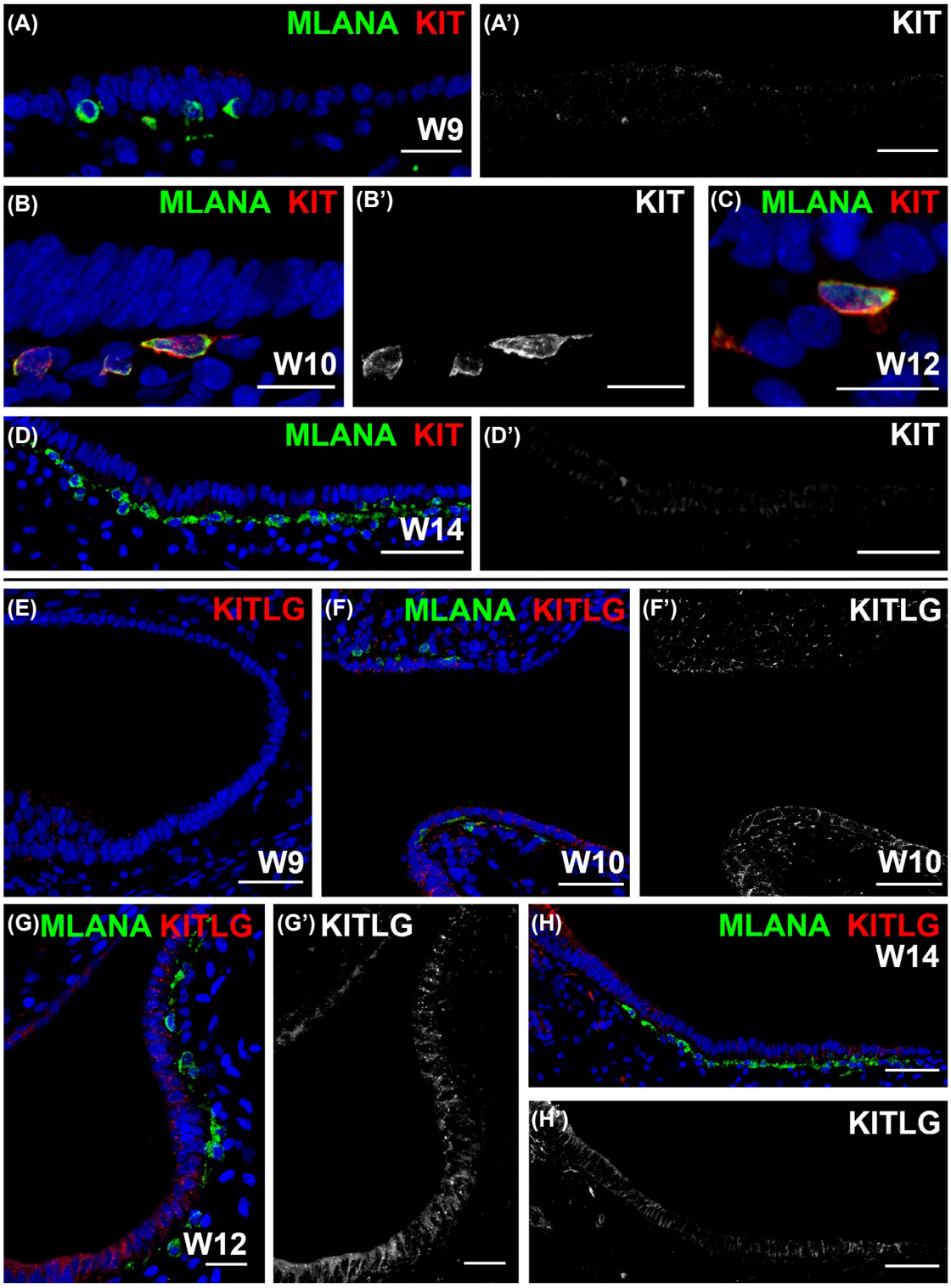


FIGURE 11 KIT and KIT ligand are temporally expressed by melanocytes and epithelia, respectively. (A-A′) At W9, melanocytes do not evidently express KIT. (B-B′) At W10, subepithelial melanocytes immunostain for KIT. (C) At W12, KIT is expressed by melanocytes. (D-D′) At W14, melanocytes in the dark cell areas do not express KIT. (E) Punctate expression of KITLG is seen in the ampullar sensory domain at W9. (F-F′) KITLG expression is seen as a punctated pattern in the periotic mesenchyme and membranous immunostaining in the dark cells. (G-G′) Dark cells surrounding the ampulla strongly express KITLG. In addition, hair cells and nerve fibers also show immunostaining of KITLG. (H-H′) Ampullar dark cells show basolateral expression of KITLG. Green: MLANA; red: KIT (A–D), KITLG (E–H); and blue: DAPI. Scale bars: 15 μm (C), 20 μm (B), and 50 μm (A, D, and E–H)

of the otic vesicle and abundantly aligning the neural tube epithelium. Previous lineage tracing experiments in mouse models have not seen the spatial pattern of melanoblasts in the neural tube and inner ear as described here (Adameyko et al., 2012; Cable et al., 1995). Even though both MITF and DCT are considered to be specific melanoblast makers, it has also been suggested that MITF plays a role in cell regulation and division in melanomas (Giuliano et al., 2010; Strub et al., 2011). Intriguingly, all observed $MITF^+$ and DCT^+ cells at W5 were found to be in mitosis based upon their DAPI staining pattern. In these sections, no $MITF^-$ or DCT^- cells could be found that were in mitosis. In control experiments using adult human skin samples, normal staining patterns in the dermal and epidermal layers were found with both these antibodies (data not shown). Together these observations could indicate that both MITF and DCT play an as yet unknown role in human fetal cell division at this developmental stage. Next, we immunostained for additional melanocyte-lineaged markers: SOX10, PAX3, and MLANA. SOX10 is expressed by immature and mature glial cells and melanocytes, whereas PAX3 and MLANA are specifically expressed by melanocyte-lineaged cells. Interestingly, we found a population of $SOX10^+PAX3^+MLANA^+$ cells between the otic vesicle and the outgrowth of the glossopharyngeal nerve, at the location of rhombomere 6. $SOX10^+$ glial (progenitor) cells located in the developing facial, vestibulocochlear, and glossopharyngeal nerves did not express PAX3, nor MLANA. Also, $SOX10^-PAX3^+MLANA^+$ cells were not seen around the facial or vestibulocochlear nerves. Therefore, we believe that the $SOX10^+PAX3^+MLANA^+$ cells correctly represent the neural-crest-derived melanoblast population. Even though we did not perform tracing experiments, these findings support the hypothesis that inner ear melanocytes might originate from a different neural crest source than the inner ear glial cells. Glial cells populate the inner ear via the facio-acoustic ganglionic complex (D'Amico-Martel & Noden, 1983; Locher et al., 2014; Sandell et al., 2014). Our current observations could indicate that inner ear melanocytes originate from the region of rhombomere 6, at the other side of the otic vesicle, which is in line with the observation that early distribution of melanoblasts is seen caudally from the otic vesicle in mice (Steel et al., 1992).

4.2 | Spatiotemporal development

During the development of the inner ear, the vestibular organs start to develop at an earlier stage than the cochlea, which is grossly reflected in a lead of 2–3 weeks in humans (for a review, see Lim & Brichta, 2016). A similar spatiotemporal development is seen in the present study as melanocytes were associated with vestibular epithelia around W7, whereas melanocytes associated with cochlear epithelia in the lateral wall of the basal turn were not observed before W10 (Locher et al., 2015).

The dark cell epithelium is biochemically and morphologically homologous to the marginal cell layer in the stria vascularis, expressing the same set of ion channels and -pumps that contribute to endolymph homeostasis (Bartolami et al., 2011; Kimura, 1969; Locher et al., 2015; Nicolas et al., 2001; Wangemann, 2002). In the adult inner ear, underlying both dark cells and marginal cells is a tight layer of melanocytes, which play a pivotal role in K^+ recycling and endolymph homeostasis (Marcus et al., 2002; Wangemann, 2002). Interestingly, we found that in immature vestibular organs, melanocytes are not only closely associated with dark cell epithelium, but with the transitional zone as well. This changes in later stages, during which melanocytes are confined to the dark cell areas. In mice, immature dark cells require the assistance of transitional cells to secrete K^+ into the endolymph, which changes when dark cells mature and become the primary source of K^+ secretion (Bartolami et al., 2011). We observed the same developmental pattern in human samples. Expression of Na^+/K^+-ATPase α1 becomes gradually visible in all vestibular epithelia between W7 and W8, followed by spatial confinement to the dark cell epithelium around W11. As such, the interaction between melanocytes and transitional cells during early human fetal development might be essential for endolymph production.

4.3 | Saccular melanocytes

Only a handful of studies describe the presence of melanocytes around the adult saccule of humans (Wolf, 1931) and other mammalian species (Kim et al., 2019; Kimura, 1969; LaFerriere et al., 1974; Zhang et al., 2013). In our study, no melanocytes were seen migrating through the saccular periotic mesenchyme nor were they found to be associated with saccular epithelia from W7 until W14. In fact, no melanocytes were observed throughout the entire inner ear periotic mesenchyme between W11 and W14, indicating at least to some extent that migration has completed. In addition, the human study from Wolf (1931) describing the presence of melanocytes around the saccule does not support this statement with evidence. We, therefore, hypothesize that melanocytes are not present in or around the human saccule during fetal development nor in the healthy adult inner ear.

4.4 | Epithelial fold melanocytes

Epithelial folds, protrusions of epithelium into the lumen of the vestibular system, separate the individual vestibular organs

(Kawamoto & Altmann, 1967). In this study, we found that the epithelial folds separating the ampullae and utricle contain a substantial number of melanocytes. These melanocytes align with epithelial cells that strongly express Na^+/K^+-ATPase α1. As the combination of these cell types and ion transporter protein expression is characteristic for the dark cell areas, this suggests that these epithelial folds are not only important for the compartmentalization of individual vestibular organs, but have a biochemical function as well. Possibly, the presence of these epithelial folds leads to an enlarged active surface area, thereby increasing exchange of ions and contributing to endolymph homeostasis.

4.5 | Dark cell basement membrane

Previous studies on the interaction between melanocytes and dark cells in human vestibular organs has shown spindle-shaped melanocytic dendrites in between the epithelial cells lining the lumen (i.e., dark cells), indicating penetration of the local basement membrane (Masuda et al., 1994, 1995, 1996, 1997), similar to what is seen during the development of the marginal and intermediate cells of the stria vascularis in the cochlea (Locher et al., 2015). To better clarify the association between melanocytes and dark cells during human fetal development, we immunostained for laminin. At the later fetal stages, laminin staining between melanocytes and dark cells demonstrated an irregular and interrupted staining pattern and was even absent in some areas. Our findings of an interrupted component of the basement membrane are in line with earlier observations on the tight interaction between melanocytic dendrites and dark cells.

4.6 | Melanoblasts and dark cell epithelia express migration-related cadherins

Cadherins play an important role in mediating the interaction between migrating neural crest cells and their microenvironment (Pla et al., 2001). Developmental studies with mice found a distinct, temporal expression pattern of ECAD and PCAD in the migration of melanoblasts toward and within the skin (Nishimura et al., 1999). At day E11.5, melanoblasts were $ECAD^-PCAD^-$, but over the course of several days the expression pattern of both cadherins diversified into three region-specific subpopulations of melanocytes, with expression patterns matching those in surrounding cells: dermal melanocytes were $ECAD^-PCAD^-$, epidermal melanocytes were $ECAD^{high}PCAD^{low}$ and follicular melanocytes were $ECAD^-PCAD^{medium/high}$ (Nishimura et al., 1999). Our results show an equally interesting trend in expression of these cadherins: inner ear melanoblasts are $ECAD^+PCAD^+$ at W5, seem to express less PCAD at W10, and are $ECAD^+PCAD^-$ at W14, mostly resembling the expression pattern of mouse epidermal melanocytes. As expected, their target locations express the same patterns, with an intense immunostaining for ECAD and a lack of PCAD in the epithelial dark cells at W14. Moreover, prior to penetrating the basement membrane separating the dermis and epidermis, mice melanoblasts express ECAD. It was hypothesized that the transit from dermal to epidermal is made possible by the ability of ECAD to induce metalloproteinase activity and resulting in disruption of the basement membrane, enabling melanocyte migration (Delmas et al., 1999). In light of our finding that the basement membrane is locally disrupted underneath dark cell epithelia, we believe it is worth investigating the surmised metalloproteinase activity of inner ear melanocytes.

4.7 | Vestibular melanocytes and dark cell epithelia express KIT and KITLG, respectively

KIT and its ligand KITLG have been extensively investigated for their roles in migration, survival, and proliferation of epidermal melanocytes (for reviews, see Yoshida et al., 2001; Wehrle-Haller, 2003). KITLG, also known as stem cell factor or steel factor, exists in both a transmembrane and soluble form. To investigate a possible role of the KIT/KITLG axis in migration and targeting of inner ear melanocytes, we immunostained for both proteins. We hypothesized that dark cells express the membranous and/or soluble KITLG to guide KIT^+ melanocytes toward their destination underneath the dark cell epithelium. Interestingly, only at W10 and W12 melanocytes are KIT^+, whereas at W9 or W14 no KIT has been observed in vestibular melanocytes. This temporal expression pattern seems to correspond with that of KITLG. At W9, only punctate immunostaining was visible in the epithelia, whereas at W10, KITLG was visible in the membranes of dark cells and punctated in the periotic mesenchyme, the latter presumably being the soluble protein. The most notable expression of KITLG in dark cell epithelia was seen at W12, showing membranal staining and a strong punctated expression pattern of surmised soluble KITLG. At W14, expression of KITLG is seen as membranal staining. In addition, from W12 and onwards, nerve fibers and hair cells also showed expression of KITLG. Although speculating about the function of the KIT/KITLG expression in nerve fibers and hair cells is beyond the scope of this study, we believe our observations support the suggestion that this axis is involved in guiding of KIT^+ melanocytes toward the $KITLG^+$ dark cell epithelium.

4.8 | Clinical relevance

In humans, pigmentation anomalies can be associated with inner ear dysfunction and malformations, resulting in hearing loss and balance disorders. Waardenburg syndrome, the most common form of autosomal dominant sensorineural hearing loss, can be divided into four subtypes and is caused by

disturbed migration, proliferation, survival, or differentiation of several cell types, including neural-crest-derived melanocytes (Pingault et al., 2010). Type I and Type II Waardenburg are caused by mutations in genes specifically expressed by melanocyte-lineaged cells (e.g., mutations in *PAX3* cause type I; mutations in *MITF* cause type II). In healthy subjects, strial melanocytes play a pivotal role in generation of the endocochlear potential, which is essential in hearing. Mutations in the melanocyte lineage could hence be responsible for hearing loss. Interestingly, patients with type I and type II Waardenburg frequently experience vestibular symptoms such as vertigo and dizziness, but these are much less investigated or understood (Black et al., 2001). We hypothesize that, in analogy to cochlear melanocytes and hearing loss, vestibular melanocytes are related to or responsible for vestibular symptoms in these patients due to a disturbed potassium recycling.

5 | Conclusion

In this article, we have described for the first time the development and spatiotemporal pattern of vestibular melanocytes in the human embryonic and fetal inner ear. Melanoblasts are first seen caudally from the otic vesicle at W5 and express migration-related cadherins. Over the course of several weeks, melanocytes are observed throughout the (pre-)periotic mesenchyme, underneath the vestibular epithelia lining the endolymphatic lumen and finally underneath the vestibular dark cell epithelia. Understanding this complex process of migration and fate of vestibular melanocytes could further our insight into normal vestibular function and pathophysiological mechanisms underlying vestibular disorders, especially those associated with pigmentation anomalies.

ACKNOWLEDGMENTS

The authors are very grateful for the collaboration between our department and Mildred Clinics (locations Arnhem and Eindhoven, the Netherlands). Both medical and supporting staff have provided us with invaluable support in obtaining legal permission and collecting specimens. The authors thank A.M.A. Boonzaier-Van der Laan and L.M. Voortman from the Department of Cell and Chemical Biology of the Leiden University Medical Center for their help with image acquisition and deconvolution. This work was supported by the Hoogenboom-Beckfonds foundation.

CONFLICT OF INTEREST

The authors have no conflict of interest to declare.

AUTHOR CONTRIBUTIONS

All authors had full access to all the data in the study and have read and approved the final version of the manuscript. *Conceptualization:* E.V.B., J.D.G., H.L., and P.P.V.B.; *Methodology:* E.V.B., W.V.D.V., J.D.G., H.L., and P.P.V.B.; *Formal analysis:* E.V.B., J.D.G., H.L., and P.P.V.B.; *Investigation:* E.V.B. and W.V.D.V.; *Resources:* E.V.B., E.H., and H.L.; *Writing:* E.V.B., W.V.D.V., J.D.G., E.H., H.L., and P.P.V.B.

DATA AVAILABILITY STATEMENT

All raw data and separate channels of merged images will be freely shared upon request.

ORCID

Edward S. A. van Beelen https://orcid.org/0000-0002-6952-9098
Erik F. Hensen https://orcid.org/0000-0002-4393-7421
Heiko Locher https://orcid.org/0000-0002-4174-0270

REFERENCES

Adameyko, I., Lallemend, F., Aquino, J. B., Pereira, J. A., Topilko, P., Müller, T., Fritz, N., Beljajeva, A., Mochii, M., Liste, I., Usoskin, D., Suter, U., Birchmeier, C., & Ernfors, P. (2009). Schwann cell precursors from nerve innervation are a cellular origin of melanocytes in the skin. *Cell*, *139*, 366–379. https://doi.org/10.1016/j.cell.2009.07.049

Adameyko, I., Lallemend, F., Furlan, A., Zinin, N., Aranda, S., Kitambi, S. S., Blanchart, A., Favaro, R., Nicolis, S., Lübke, M., Müller, T., Birchmeier, C., Suter, U., Zaitoun, I., Takahashi, Y., & Ernfors, P. (2012). Sox2 and Mitf cross-regulatory interactions consolidate progenitor and melanocyte lineages in the cranial neural crest. *Development*, *139*, 397–410. https://doi.org/10.1242/dev.065581

Barozzi, S., Ginocchino, D., Socci, M., Alpini, D., & Cesarani, A. (2015). Audiovestibular disorders as autoimmune reaction in patients with melanoma. *Medical Hypotheses*, *85*, 336–338. https://doi.org/10.1016/j.mehy.2015.06.009

Bartolami, S., Gaboyard, S., Quentin, J., Travo, C., Cavalier, M., Barhanin, J., & Chabbert, C. (2011). Critical roles of transitional cells and Na/K-ATPase in the formation of vestibular endolymph. *Journal of Neuroscience*, *31*, 16541–16549. https://doi.org/10.1523/JNEUROSCI.2430-11.2011

Black, F. O., Pesznecker, S. C., Allen, K., & Gianna, C. (2001). A vestibular phenotype for Waardenburg syndrome? *Otology & Neurotology*, *22*, 188–194. https://doi.org/10.1097/00129492-200103000-00012

Cable, J., Jackson, I. J., & Steel, K. P. (1995). Mutations at the W locus affect survival of neural crest-derived melanocytes in the mouse. *Mechanisms of Development*, *50*, 139–150. https://doi.org/10.1016/0925-4773(94)00331-G

Cable, J., & Steel, K. P. (1991). Identification of two types of melanocyte within the stria vascularis of the mouse inner ear. *Pigment Cell Research*, *4*, 87–101. https://doi.org/10.1111/j.1600-0749.1991.tb00320.x

Ciuman, R. R. (2009). Stria vascularis and vestibular dark cells: Characterization of main structures responsible for inner-ear homeostasis, and their pathophysiological relations. *Journal of Laryngology and Otology*, *123*, 151–162. https://doi.org/10.1017/S0022215108002624

Conlee, J. W., Parks, T. N., Schwartz, I. R., & Creel, D. J. (1989). Comparative anatomy of melanin pigment in the stria vascularis. Evidence for a distinction between melanocytes and intermediate

cells in the cat. *Acta Oto-Laryngologica*, *107*, 48–58. https://doi.org/10.3109/00016488909127478

Coppens, A. G., Salmon, I., Heizmann, C. W., Kiss, R., & Poncelet, L. (2003). Postnatal maturation of the dog stria vascularis? An immunohistochemical study. *The Anatomical Record*, *270A*, 82–92. https://doi.org/10.1002/ar.a.10009

Coppens, A. G., Salmon, I., Heizmann, C. W., & Poncelet, L. (2004). Dark-cell areas in the dog vestibular endorgans: An immunohistochemical study. *Histology and Histopathology*, *19*, 1227–1235. https://doi.org/10.14670/HH-19.1227

D'Amico-Martel, A., & Noden, D. M. (1983). Contributions of placodal and neural crest cells to avian cranial peripheral ganglia. *The American Journal of Anatomy*, *166*, 445–468. https://doi.org/10.1002/aja.1001660406

De Fraissinette, A., Felix, H., Hoffmann, V., Johnsson, L. G., & Gleesom, M. J. (1993). Human Reissner's membrane in patients with age-related normal hearing and with sensorineural hearing loss. *ORL*, *55*, 68–72. https://doi.org/10.1159/000276381

Delmas, V., Pla, P., Feracci, H., Thiery, J. P., Kemler, R., & Larue, L. (1999). Expression of the cytoplasmic domain of E-cadherin induces precocious mammary epithelial alveolar formation and affects cell polarity and cell-matrix integrity. *Developmental Biology*, *216*, 491–506. https://doi.org/10.1006/dbio.1999.9517

Escobar, C., Zuast, A., Ferrer, C., & Garcia-Ortega, F. (1995). Melanocytes in the stria vascularis and vestibular labyrinth of the Mongolian Gerbil (*Meriones unguiculatus*). *Pigment Cell Research*, *8*, 271–278. https://doi.org/10.1111/j.1600-0749.1995.tb00674.x

Etchevers, H. C., Dupin, E., & Le Douarin, N. M. (2019). The diverse neural crest: From embryology to human pathology. *Development*, *146*, dev169821. https://doi.org/10.1242/dev.169821

Felix, H., De Fraisinette, A., Johnsson, L. G., & Gleeson, M. J. (1993). Morphological features of human Reissner's membrane. *Acta Oto-Laryngologica*, *113*, 321–325. https://doi.org/10.3109/00016489309135817

Franz, P., Aharinejad, S., & Firbas, W. (1990). Melanocytes in the modiolus of the guinea pig cochlea. *Acta Oto-Laryngologica*, *109*, 221–227. https://doi.org/10.3109/00016489009107437

Freyer, L., Aggarwal, L., & Morrow, B. E. (2011). Dual embryonic origin of the mammalian otic vesicle forming the inner ear. *Development*, *138*, 5403–5414. https://doi.org/10.1242/dev.069849

Fukazawa, K., Sakagami, M., Umemoto, M., Fujita, H., & Matsunaga, T. (1993). Electron microscopical observations of melanin in the endolymphatic sac. *Acta Oto-Laryngologica*, *113*(Suppl. 501), 72–75. https://doi.org/10.3109/00016489309126219

Fukazawa, K., Sakagami, M., Umemoto, M., & Senda, T. (1994). Development of melanosomes and cytochemical observation of tyrosinase activity in the inner ear. *ORL*, *56*, 247–252. https://doi.org/10.1159/000276667

Furlan, A., & Adameyko, I. (2018). Schwann cell precursor: A neural crest cell in disguise? *Developmental Biology*, *444*, S25–S35. https://doi.org/10.1016/j.ydbio.2018.02.008

Giuliano, S., Cheli, Y., Ohanna, M., Bonet, C., Beuret, L., Bille, K., Loubat, A., Hofman, V., Hofman, P., Ponzio, G., Bahadoran, P., Ballotti, R., & Bertolotto, C. (2010). Microphthalmia-associated transcription factor controls the DNA damage response and a lineage-specific senescence program in melanomas. *Cancer Research*, *70*, 3813–3822. https://doi.org/10.1158/0008-5472.CAN-09-2913

Glueckert, R., Johnson Chacko, L., Rask-Andersen, H., Liu, W., Handschuh, S., & Schrott-Fischer, A. (2018). Anatomical basis of drug delivery to the inner ear. *Hearing Research*, *368*, 10–27. https://doi.org/10.1016/j.heares.2018.06.017

Gussen, R. (1978). Melanocyte system of the endolymphatic duct and sac. *The Annals of Otology, Rhinology, and Laryngology*, *87*, 175–179. https://doi.org/10.1177/000348947808700205

Hilding, D. A., & Ginzberg, R. D. (1977). Pigmentation of the stria vascularis. The contribution of neural crest melanocytes. *Acta Oto-Laryngologica*, *84*, 24–37. https://doi.org/10.3109/00016487709123939

Igarashi, Y. (1989). Submicroscopic study of the vestibular dark cell area in human fetuses. *Acta Oto-Laryngologica*, *107*, 29–38. https://doi.org/10.3109/00016488909127476

Igarashi, Y., Takeyama, I., & Takahashi, I. (1989). Melanocytes in vestibular dark cell areas in human fetuses. *Acta Oto-Laryngologica*, *108*, 9–18. https://doi.org/10.3109/00016488909107386

Kawamoto, K., & Altmann, F. (1967). The atypical epithelial formations of the utricle. *Archives of Otolaryngology*, *85*, 561–571. https://doi.org/10.1001/archotol.1967.00760040563020

Kikuchi, T., Adams, J. C., Paul, D. L., & Kimura, R. S. (1994). Gap junction systems in the rat vestibular labyrinth: Immunohistochemical and ultrastructural analysis. *Acta Oto-Laryngologica*, *114*, 520–528. https://doi.org/10.3109/00016489409126097

Kim, Y. Y., Chao, J. R., Kim, C., Kang, T. C., Park, H. S., Chang, J., Suh, J. G., & Lee, J. H. (2019). Applicability of vital staining and tissue clearance to vascular anatomy and melanocytes' evaluation of temporal bone in six laboratory species. *Anatomia Histologia and Embryologia*, *48*, 296–305. https://doi.org/10.1111/ahe.12440

Kimura, R. S. (1969). Distribution, structure, and function of dark cells in the vestibular labyrinth. *The Annals of Otology, Rhinology, and Laryngology*, *78*, 542–561. https://doi.org/10.1177/000348946907800311

LaFerriere, K. A., Arenberg, I. K., Hawkins, J. E., & Johnsson, L. G. (1974). Melanocytes of the vestibular labyrinth and their relationship to the microvasculature. *The Annals of Otology, Rhinology, and Laryngology*, *83*, 685–694. https://doi.org/10.1177/000348947408300518

Lavezzo, M. M., Sakata, V. M., Morita, C., Rodriguez, E. E. C., Abdallah, S. F., Da Silva, F. T. G., Hirata, C. E., & Yamamoto, J. H. (2016). Vogt-Koyanagi-Harada disease: Review of a rare autoimmune disease targeting antigens of melanocytes. *Orphanet Journal of Rare Diseases*, *11*, 1–21. https://doi.org/10.1186/s13023-016-0412-4

Lim, R., & Brichta, A. M. (2016). Anatomical and physiological development of the human inner ear. *Hearing Research*, *338*, 9–21. https://doi.org/10.1016/j.heares.2016.02.004

Locher, H., de Groot, J. C. M. J., van Iperen, L., Huisman, M. A., Frijns, J. H. M., de Sousa, C., & Lopes, S. M. (2014). Distribution and development of peripheral glial cells in the human fetal cochlea. *PLoS ONE*, *9*, e88066. https://doi.org/10.1371/journal.pone.0088066

Locher, H., De Groot, J. C. M. J., Van Iperen, L., Huisman, M. A., Frijns, J. H. M., de Sousa, C., & Lopes, S. M. (2015). Development of the stria vascularis and potassium regulation in the human fetal cochlea: Insights into hereditary sensorineural hearing loss. *Developmental Neurobiology*, *75*, 1219–1240. https://doi.org/10.1002/dneu.22279

Locher, H., Frijns, J. H. M., van Iperen, L., de Groot, J. C. M. J., Huisman, M. A., de Sousa, C., & Lopes, S. M. (2013). Neurosensory development and cell fate determination in the human cochlea. *Neural Development*, *8*, 1–13. https://doi.org/10.1186/1749-8104-8-20

Marcus, D. C., & Wangemann, P. (2010). Chapter 7: Inner ear fluid homeostasis. In P.A. Fuchs editor *Oxford handbook of auditory science* (pp. 213–230). OUP Oxford.

Marcus, D. C., Wu, T., Wangemann, P., & Kofuji, P. (2002). KCNJ10 (Kir4.1) potassium channel knockout abolishes endocochlear potential. *American Journal of Physiology. Cell Physiology*, *282*, C403–C407. https://doi.org/10.1152/ajpcell.00312.2001

Masuda, M., Yamazaki, K., Kanzaki, J., & Hosoda, Y. (1994). Ultrastructure of melanocytes in the dark cell area of human vestibular organs. Functional implications of gap junctions, isolate cilia and annulate lamellae. *Anatomical Record*, *240*, 481–491. https://doi.org/10.1002/ar.1092400406

Masuda, M., Yamazaki, K., Kanzaki, J., & Hosoda, Y. (1995). Ultrastructural evidence of cell communication between epithelial dark cells and melanocytes in vestibular organs of the human inner ear. *Anatomical Record*, *242*, 267–277. https://doi.org/10.1002/ar.1092420217

Masuda, M., Yamazaki, K., Kanzaki, J., & Hosoda, Y. (1996). Ultrastructural recognition of gap junctions between melanocytes in human vestibular organs by tannic acid containing fixative preparation and freeze-fracture technique. *Anatomical Record*, *246*, 8–14. https://doi.org/10.1002/(SICI)1097-0185(199609)246:1<8:AID-AR2>3.0.CO;2-R

Masuda, M., Yamazaki, K., Kanzaki, J., & Hosoda, Y. (1997). Immunohistochemical and ultrastructural investigation of the human vestibular dark cell area: Roles of subepithelial capillaries and T lymphocyte-macrophage interaction in an immune surveillance system. *Anatomical Record*, *249*, 153–162. https://doi.org/10.1002/(SICI)1097-0185(199710)249:2<153:AID-AR1>3.0.CO;2-Z

Nicolas, M., Demêmes, D., Martin, A., Kupershmidt, S., & Barhanin, J. (2001). KCNQ1/KCNE1 potassium channels in mammalian vestibular dark cells. *Hearing Research*, *153*, 132–145. https://doi.org/10.1016/S0378-5955(00)00268-9

Nishimura, E., Yoshida, H., Kunisada, T., & Nishikawa, S. (1999). Regulation of E- and P-cadherin expression correlated with melanocyte migration and diversification. *Developmental Biology*, *215*, 155–166. https://doi.org/10.1006/dbio.1999.9478

Okuno, K., & Nomura, Y. (1996). Distribution of melanin in the human utricular wall. *The Showa University Journal of Medical Sciences*, *8*, 227–233. https://doi.org/10.15369/sujms1989.8.227

Opdecamp, K., Nakayama, A., Nguyen, M. T., Hodgkinson, C. A., Pavan, W. J., & Arnheiter, H. (1997). Melanocyte development in vivo and in neural crest cell cultures: Crucial dependence on the Mitf basic-helix-loop-helix-zipper transcription factor. *Development*, *124*, 2377–2386.

Palma, S., Bodrini, P., Nucci, R., Fano, R. A., Cenacchi, G., & Martini, A. (2018). Melanin in human vestibular organs: What do we know? An ultrastructural study and review of the literature. *Hearing, Balance and Communication*, *16*, 101–107. https://doi.org/10.1080/21695717.2018.1461488

Peters, T. A., Kuijpers, W., Tonnaer, E. L. G. M., Van Muijen, G. N. P., & Jap, P. H. K. (1995). Distribution and features of melanocytes during inner ear development in pigmented and albino rats. *Hearing Research*, *85*, 169–180. https://doi.org/10.1016/0378-5955(95)00043-4

Pingault, V., Ente, D., Dastot-Le Moal, F., Goossens, M., Marlin, S., & Bondurand, N. (2010). Review and update of mutations causing Waardenburg syndrome. *Human Mutation*, *31*, 391–406. https://doi.org/10.1002/humu.21211

Pla, P., Moore, R., Morali, O., Grille, S., Martinozzi, S., Delmas, V., & Larue, L. (2001). Cadherins in neural crest cell development and transformation. *Journal of Cellular Physiology*, *189*, 121–132. https://doi.org/10.1002/jcp.10008

Roberts, D. S., & Linthicum, F. H. (2015). Distribution of melanocytes in the human cochlea. *Otology & Neurotology*, *36*, e99–e100. https://doi.org/10.1097/MAO.0000000000000697

Sandell, L. L., Butler Tjaden, N. E., Barlow, A. J., & Trainor, P. A. (2014). Cochleovestibular nerve development is integrated with migratory neural crest cells. *Developmental Biology*, *385*, 200–210. https://doi.org/10.1016/j.ydbio.2013.11.009

Savin, C. (1965). The blood vessels and pigmentary cells of the inner ear. *The Annals of Otology, Rhinology, and Laryngology*, *74*, 611–623. https://doi.org/10.1177/000348946507400303

Schrott, A., & Spoendlin, H. (1987). Pigment anomaly-associated inner ear deafness. *Acta Oto-Laryngologica*, *103*, 451–457.

Schuth, O., McLean, W. J., Eatock, R. U., & Pyott, S. J. (2014). Distribution of Na, K-ATPase α subunits in rat vestibular sensory epithelia. *Journal of the Association for Research in Otolaryngology*, *15*, 739–754. https://doi.org/10.1007/s10162-014-0479-3

Steel, K. P., & Barkway, C. (1989). Another role for melanocytes: Their importance for normal stria vascularis development in the mammalian inner ear. *Development*, *107*, 453–463. https://doi.org/10.1016/0168-9525(90)90041-4

Steel, K. P., Barkway, C., & Bock, G. R. (1987). Strial dysfunction in mice with cochlea-saccular abnormalities. *Hearing Research*, *27*, 11–26. https://doi.org/10.1016/0378-5955(87)90022-0

Steel, K. P., Davidson, D. R., & Jackson, I. J. (1992). TRP-2/DT, a new early melanoblasts marker, shows that steel growth factor (c-kit ligand) is a survival factor. *Development*, *115*, 1111–1119.

Strub, T., Giuliano, S., Ye, T., Bonet, C., Keime, C., Kobi, D., Le Gras, S., Cormont, M., Ballotti, R., Bertolotto, C., & Davidson, I. (2011). Essential role of microphthalmia transcription factor for DNA replication, mitosis and genomic stability in melanoma. *Oncogene*, *30*, 2319–2332. https://doi.org/10.1038/onc.2010.612

Ten Cate, W. J., Curtis, L. M., & Rarey, K. E. (1994). Na, K-ATPase α and β subunit isoform distribution in the rat cochlear and vestibular tissues. *Hearing Research*, *75*, 151–160. https://doi.org/10.1016/0378-5955(94)90066-3

Wakaoka, T., Motohashi, T., Hayashi, H., Kuze, B., Aoki, M., Mizuta, K., Kunisada, T., & Ito, Y. (2013). Tracing sox10-expressing cells elucidates the dynamic development of the mouse inner ear. *Hearing Research*, *302*, 17–25. https://doi.org/10.1016/j.heares.2013.05.003

Wangemann, P. (2002). K^+ cycling and the endocochlear potential. *Hearing Research*, *165*, 1–9. https://doi.org/10.1016/s0378-5955(02)00279-4

Wehrle-Haller, B. (2003). The role of Kit-ligand in melanocyte development and epidermal homeostasis. *Pigment Cell Research*, *16*, 287–296. https://doi.org/10.1034/j.1600-0749.2003.00055.x

Wolf, D. (1931). Melanin in the inner ear. *Archives of Otolaryngology*, *14*, 195–211.

Wright, C. G., & Lee, D. H. (1989). Pigmented cells of the stria vascularis and spiral ligament of the chinchilla. *Acta Oto-Laryngologica*, *108*, 190–200. https://doi.org/10.3109/00016488909125518

Yoshida, H., Kinisada, T., Grimm, T., Nishimura, E., Nishioka, E., & Nishikawa, S. (2001). Review: Melanocyte migration and survival controlled by SCF/c-kit expression. *The Journal of Investigative Dermatology Symposium Proceedings*, *6*, 1–5. https://doi.org/10.1046/j.0022-202x.2001.00006.x

Zhang, F., Zhang, J., Neng, L., & Shi, X. (2013). Characterization and inflammatory response of perivascular-resident macrophage-like melanocytes in the vestibular system. *Journal of the Association for Research in Otolaryngology*, *14*, 635–643. https://doi.org/10.1007/s10162-013-0403-2

Zhang, W., Dai, M., Fridberger, A., Hassan, A., Degagne, J., Neng, L., Zhang, F., He, W., Ren, T., Trune, D., Auer, M., & Shi, X. (2012). Perivascular-resident macrophage-like melanocytes in the inner ear

are essential for the integrity of the intrastrial fluid–blood barrier. *Proceedings of the National Academy of Sciences of the United States of America*, *109*, 10388–10393. https://doi.org/10.1073/pnas.1205210109

SUPPORTING INFORMATION

Additional Supporting Information may be found online in the Supporting Information section.

How to cite this article: van Beelen ESA, van der Valk WH, de Groot JCMJ, Hensen EF, Locher H, van Benthem PPG. Migration and fate of vestibular melanocytes during the development of the human inner ear. *Develop Neurobiol*. 2020;00:1–22. https://doi.org/10.1002/dneu.22786